Integrated Arctic Observation System

Research and Innovation Action under EC Horizon 2020
Grant Agreement no. 727890

Project coordinator:
Nansen Environmental and Remote Sensing Center, Norway

Deliverable 2.2

Report on exploitation of existing data: ocean and sea ice data

Start date of project:	01 December 2016	Duration:	60 months
Due date of deliverable:	31 May 2018	Actual submission date:	31 May 2018
Lead beneficiary for preparing the deliverable:		NERSC	
Person-months used to produce deliverable:		8.5 + pm	

Authors: Hanne Sagen, Torill Hamre, Espen Storheim, Azuka Yamakawa, Brian Dushaw, Stein Sandven, Roberta Pirazzini, Ingo Schewe, Thomas Soltwedel, Axel Behrendt, Carsten Ankjær Ludwigsen, Ole B. Andersen, Agnieszka Beszczynska-Möller, Waldemar Walczowski, Michel K. Sejr, Andrew King, Philip Wallhead, Fanny Ardhuin, Georg Heygster, Kuvvet Atakan, Mathilde Sørensen

Version	DATE	CHANGE RECORDS	LEAD AUTHOR
1.0	30/04/2017	Template	Roberta Pirazzini
1.1	11/12/2017	1st Draft	
1.2	31/05/2018	Final version	H. Sagen

Approval	31.05.2018	Sign.  coordinator

USED PERSON-MONTHS FOR THIS DELIVERABLE					
No	*Beneficiary*	*PM*	*No*	*Beneficiary*	*PM*
1	NERSC	***1.5***	**24**	Terradue	
2	UiB	***x***	**25**	GINR	
3	IMR		**26**	UNEXE	
4	MISU		**27**	NIVA	***1.2***
5	AWI	***1.5***	**28**	CNRS	
6	IOPAN	***0.7***	**29**	U Helsinki	
7	DTU	***0.5***	**30**	GFZ	
8	AU	***0.5***	**31**	ARMINE	
9	GEUS		**32**	IGPAN	
10	FMI		**33**	U SLASKI	
11	UNIS	***0.1***	**34**	BSC	
12	NORDECO		**35**	DNV GL	
13	SMHI		**36**	RIHMI-WDC	
14	USFD		**37**	NIERSC	
15	NUIM		**38**	WHOI	
16	IFREMER	***1.5***	**39**	SIO	
17	MPG		**40**	UAF	
18	EUROGOOS		**41**	U Laval	
19	EUROCEAN		**42**	ONC	
20	UPM		**43**	NMEFC	
21	UB	***1***	**44**	RADI	
22	UHAM		**45**	KOPRI	
23	NORUT		**46**	NIPR	
			47	PRIC	

***x** = contribution to the deliverable*

DISSEMINATION LEVEL		
PU	Public, fully open	X
CO	Confidential, restricted under conditions set out in Model Grant Agreement	
CI	Classified, information as referred to in Commission Decision 2001/844/EC	

EXECUTIVE SUMMARY

This report presents a selection of data products from existing ocean and sea ice measurements under WP2 Task 2.2 (Exploitation of existing data towards improved data products). This is done by applying various methodologies for data processing to derive of geophysical and biogeochemical quantities that can be used further work in the project, especially in WP5 (Data management and integration) and in WP6 (Applications towards stakeholders). This report is complementary to D2.1 (Report on present observing capacities and gaps: ocean and sea ice observing systems), which includes an assessment of existing data collections based on an on-line survey (https://intaros.nersc.no/node/651).

NERSC presents acoustic data from several field experiments in the Fram Strait carried out over a period of 110years. The presentation includes both active and passive acoustic data, description of how the experiments were conducted, processing steps from raw data to the resulting data products, and standardisation of formats for data and metadata.

UiB and GEUS present an earthquake cataloguefor the Arctic region (described in D2.8).

AWI presents the Unified Database for Arctic and Subarctic hydrography (UDASH), which includes all available data for the period 1980-2015. This archive is updated yearly and is available from the PANGAEA repository.

IOPAN presents a reprocessed hydrography data set for the Nordic Seas and the Fram Strait area collected by RV Oceania from 1988 to 2017 (the AREX programme). The data set is used for higher-level products such as time series of transports, heat content and dynamic topography. IOPAN also presents data from the A-TWAIN moorings north of Svalbard, deployed from 2012-2017. These data includes profiles of CTD and current data, which are used to present time series of temperature, salinity and currents. Furthermore, IOPAN presents Argo floats in the Nordic Seas and hydrographic data sets from Svalbard fjords.

DTU Space presents satellite radar altimeter products from 26 years of data in the Arctic (ERS-1/2, EnviSat and CryoSat2) showing sea level anomaly, mean sea surface height, and mean dynamic topography.

Aarhus University presents the Greenland Ecosystem Monitoring Programme, which collects an extensive range of physical, chemical and biological variables, with focus on two sampling sites: the sub-arctic Nuuk in West Greenland and high-Arctic Zackenberg in East Greenland. The programme allows both quantification of climate change and also an analysis of the potential biological consequences in both terrestrial, limnic and marine systems. For marine research, the CTD observations in Young Sound from 2003 to 2015 is important, showing changes in the water masses of the fjord.

Ifremer presents satellite sea ice drift products from CERSAT, while University of Bremen presents satellite-derived multiyear ice concentration and thin ice thickness products.

Finally, NIVA presents in situ datasets for Arctic carbonate system chemistry, nutrients, and phytoplankton biomass. The data sets include 1) surveyed existing data collections, and 2) analysed the data collections for data coverage and sampling bias.

The next step in WP2 is to select data sets and repositories to be prepared for use in the Integrated Arctic Observing System. The survey of existing systems will continue in the second half of 2018 in order to prepare a more extensive assessment of the observing systems.

Table of Contents

1. INTRODUCTION 5

2. DATA EXPLOITATION AND DATA PRODUCTS 5

2.1 NERSC 5

2.1.1 The UNDER-ICE experiment 5

2.1.2 Acoustic datasets from the UNDER-ICE experiment 6

2.1.3 Acoustic data products from ACOBAR experiment 9

2.1.4. Standardization of data formats for acoustic data 9

2.2 UiB AND GEUS: EARTHQUAKE AND FOCAL MECHANISM CATALOG OF THE ARCTIC 11

2.3 AWI 11

2.3.1 UDASH - Unified Database for Arctic and Subarctic Hydrography 11

2.4 IOPAN 13

2.4.1 AREX data collection in the Nordic Seas and Fram Strait 13

2.4.2 Processed data set from A-TWAIN Poland moorings north of Svalbard 16

2.4.3 Argo float data sets from deployments in the Nordic Seas 19

2.4.4 Hydrographic data sets from long-term monitoring in Svalbard fjords 19

2.5 DTU SPACE 20

2.5.1 Sea Level Anomaly 20

2.5.2 Mean Sea Surface 21

2.5.3 Mean Dynamic Topography 21

2.6 AARHUS UNIVERSITY 23

2.7 IFREMER 24

2.7.1 Arctic sea ice displacement from low-resolution satellite data 24

2.7.2 Arctic sea ice displacement at medium resolution from satellite data 25

2.8 UNIVERSITY OF BREMEN 27

2.8.1 Multiyear sea ice concentration product based on AMSR2 and scatterometers 27

2.8.2 Thickness of thin sea ice retrieval from L band satellite sensors SMOS and SMAP 28

2.9 NIVA 29

2.9.1 Seawater carbonate system chemistry 29

2.9.2 Seawater nutrients and phytoplankton biomass 31

3. RECOMMENDATIONS AND FURTHER WORK 34

4. REFERENCES 35

1. Introduction

This report presents a selection of data products from existing ocean and sea ice measurements under WP2 Task 2.2 (Exploitation of existing data towards improved data products). This is done by applying various methodologies for data processing to derive of geophysical and biogeochemical quantities that can be used further work in the project, especially in WP5 (Data management and integration) and in WP6 (Applications towards stakeholders). The report presents both satellite derived ocean and sea ice products as well as products from in situ observing systems. This report is complementary to D2.1 (Report on present observing capacities and gaps: ocean and sea ice observing systems). D2.1 includes an assessment of existing data collections based on responses from INTAROS partners to an on-line survey (https://intaros.nersc.no/node/651).

INTAROS has focus on in situ observing systems, so most of the efforts in WP2 are devoted to improve data processing and derived data products from the partners working Task 2.2. Regarding satellite remote sensing data, new data products are being developed from sensors that have become recently available or have long-term perspective. The remote sensing work is mostly done in other research projects and in the Copernicus services, but the results of the remote sensing work will be exploited in combination with in situ data, as described in D2.1. In WP3 of INTAROS, new data from field campaigns will be obtained in the next 1 – 2 years. These will be used in combination with data products presented in this report in the application studies in WP6.

Most of this report describes the enhanced data products provided by the project partners involved in Task 2.2 (Section 2). Recommendations for further work is discussed in Section 3.

2. Data exploitation and data products

This section includes the description of the work done on data exploitation/preparation, as well as the work to format and characterize the data (determining coverage, resolution, uncertainty, etc.) in order to be used in further work in the project (WP5 and WP6).

2.1 NERSC

In D2.1 the Fram Strait Acoustic System has been described as well as data sets from two previous experiments ACOBAR and DAMOCLES (Dushaw, 2018). In this report we describe recently developed data formats for holding the acoustic datasets, developed within NorDataNet and INTAROS (Task 2.1 and Task 2.3). Furthermore, we present the UNDER-ICE data processed as part of INTAROS and other projects. These data include ambient noise data, acoustic travel time data and ocean temperature from the travel time data.

2.1.1 The UNDER-ICE experiment

The UNDER-ICE experiment consists of five moorings, denoted UI1 to UI5, deployed in September 2014 in the Fram Strait. Fig. 1 shows the placement of the UNDER-ICE moorings, compared to the locations of the ACOBAR moorings. The contour plot illustrates the bathymetry obtained from the International Bathymetric Chart of the Arctic Ocean (IBCAO) [9]. Two of the moorings, UI2 and UI5, are equipped with Teledyne Webb Research sweeper sources that transmit 90 s linear FM sweeps from approximately 200-300 Hz. UI2 transmits every 3rd hour (0000, 0300, …, UTC) on odd year days, while UI5 transmits every 3rd hour of

every day, six minutes after UI2. Mooring UI4 is located in a region that is covered by ice in the winter, for transmissions through the marginal ice zone (MIZ).

Each mooring is equipped with 10 hydrophone modules (HM), recording a total of 130 seconds at a sampling frequency of 1953.125 kHz. The HM's are equidistantly spaced by 9 m, creating an array with an aperture of 81 m. The sources and receivers are synchronized by the DSTAR controllers. Four transponders are placed on the ocean floor in a square shape around the moorings. These are used to position the DSTAR's, sources, and HM's before and after each transmission, in three dimensions. With this mooring configuration, a total of 7 different source-receiver paths are available, ranging from 130 km (UI2-UI1) to 278 km (UI2-UI4).

The HM's are equipped with thermistors that measure the temperature at regular intervals, and the DSTAR's are equipped with calibrated pressure sensors. Moorings UI4 and UI5 are also augmented with oceanographic instruments (Sea-Bird SBE37 and SBE39) that measure the temperature, salinity, and pressure at 5 or 10 min intervals, and in total three Acoustic Doppler Current Meters (ADCP). This additional information supports the oceanographic interpretation of the acoustic results, but is not included in the Questionnare B.

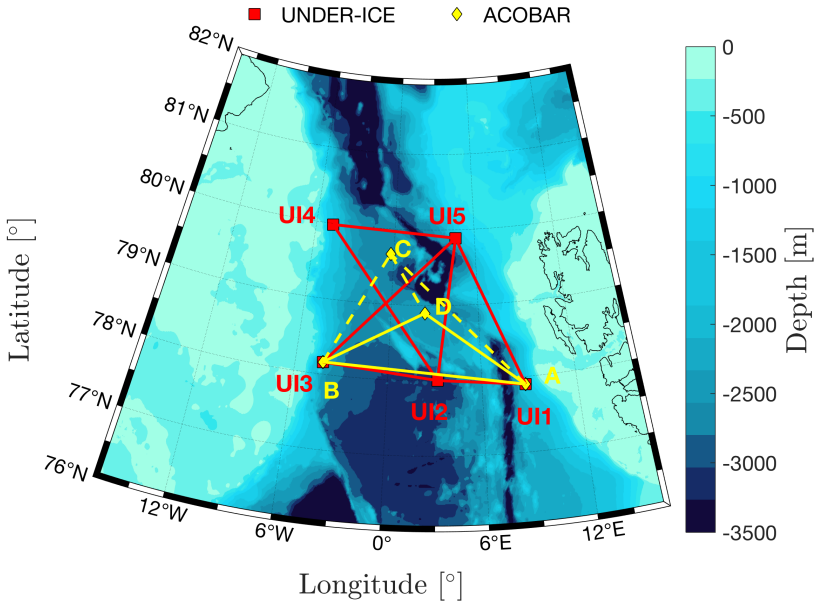

Fig. 1. Geometry of the moorings in the UNDER-ICE project (red circles, denoted UI1-UI5), compared to the ACOBAR project (yellow diamonds, denoted A-D). The contour plot indicates the bathymetry obtained from IBCAO.

2.1.2 Acoustic datasets from the UNDER-ICE experiment

Figure 1 shows a block diagram outlining the key components in the processing from hydrophone recordings to average temperature measurements. The raw data obtained from the instruments are converted to NetCDF files for the further processing. The DSTAR controller provides both recordings of the navigation signals, as well as a comparison between a low-power quartz oscillator and a high-power Rubidium oscillator. The latter is in turn used to compute a clock correction, which ensures that the timing of the instruments is correct during the experiment. Navigation recordings are also made by the HM's, which allows for positioning of the DSTAR and the individual HM's on each mooring.

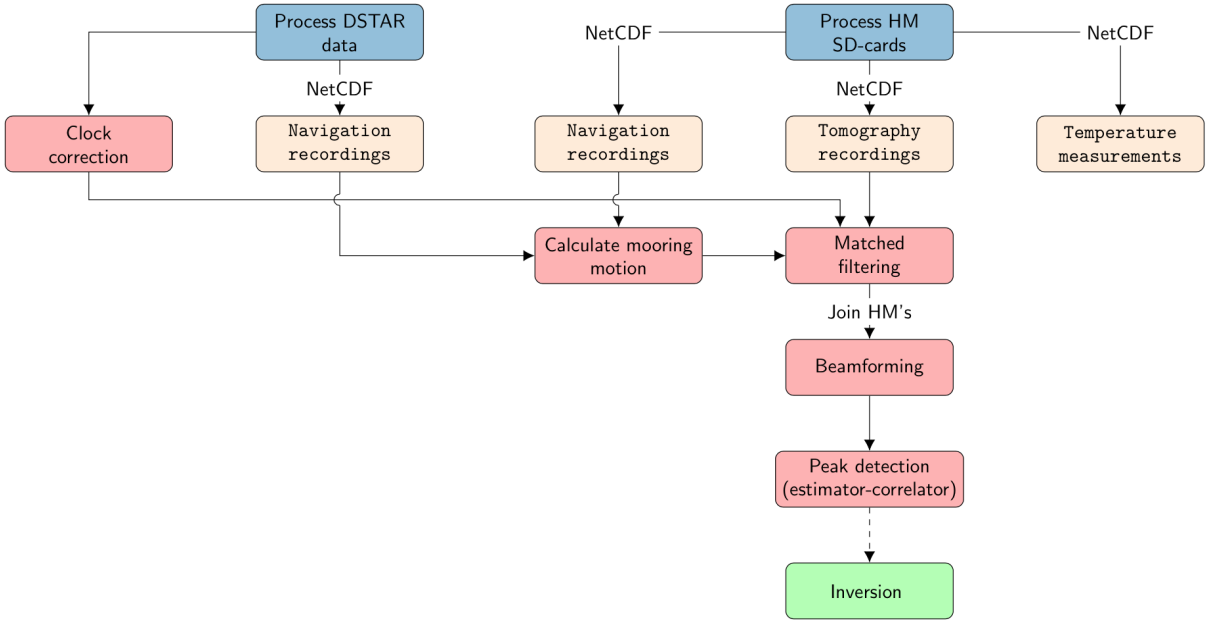

Figure 2: Block diagram of the processing of the UNDER-ICE tomography data.

Each tomography recording is processed, and the appropriate time correction terms and the calibration (frequency response) are applied. The signals are then matched-filtered by cross-correlating the recorded waveform with a synthetic version of the transmitted signal, which in turn compresses the 90 s linear frequency sweep into a pulse of approximately 10 ms duration and increases the signal-to-noise ratio. Only the first 30 s of the recordings are kept, in order to reduce the computational time.

The HM's are spaced by 9 m on the mooring wire, thus creating a receiver array with an 81 m aperture. This configuration allows beamforming to be used, which provides information about the angles of the different arrivals at the receiver. Beamforming is done on the output of the matched-filter associated with each transmission. The estimator-correlator (EC) is in turn used to detect the potential peaks associated with arrivals (Dzieciuch, 2014; Sagen *et al*., 2017). The inversion method from travel time to depth- and range-average temperature determines the coherence values used in the EC: large coherence values are needed for the random-method (Dushaw & Sagen, 2017); while smaller values are required for the traditional method where arrivals are associated with specific rays (Munk *et al*., 1995).

Figure 2 shows an example of the processing of actual data from the UNDER-ICE experiment. The time-domain recording obtained from the upper hydrophone on UI4 is shown in (a), and the corresponding spectrogram is presented in (b). In addition to the tomography signals, these recordings contain valuable information about the soundscape in the region of the acoustic network. The magnitude of the matched-filter output is shown in (c). The 90 s long sweep is now compressed into a short pulse, seen approximately 20 s after the start of the recording. In (d), the matched-filter output from each HM is combined and shown as a function of depth, and the time is relative to the start of the transmission. The beamformed data is shown in (e) as a function of travel time and arrival angle (relative to the horizontal). The dot-plot shown in (f), shows the arrivals as a function of transmission date, travel time, and arrival angle, which are selected after processing with the estimator-correlator with large coherence values, SNR filtering (lower threshold set to 25 dB), and a side-lobe-filter.

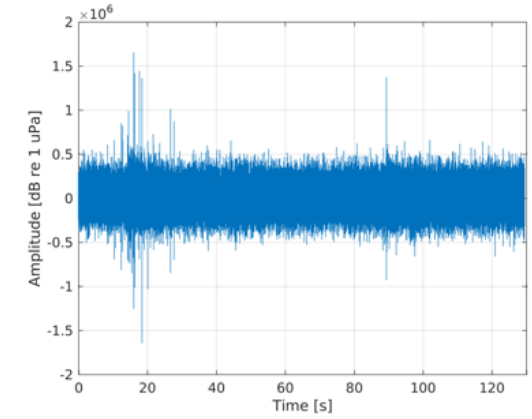

(a)

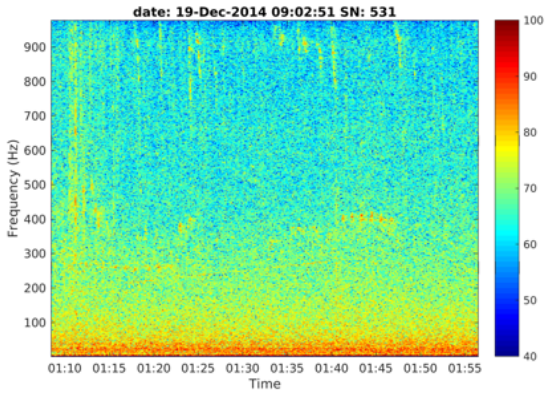

(b)

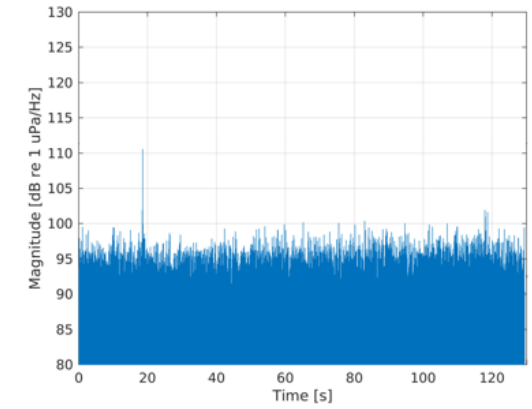

(c)

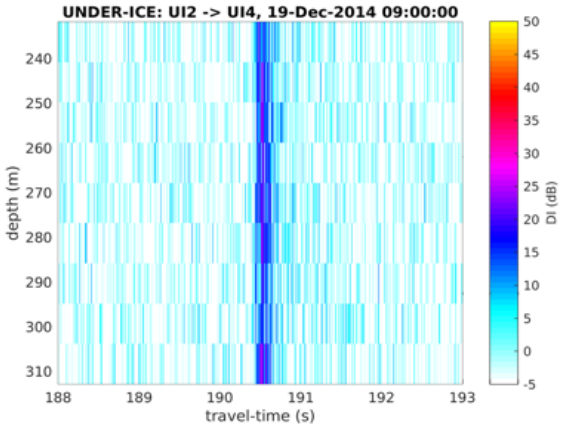

(d)

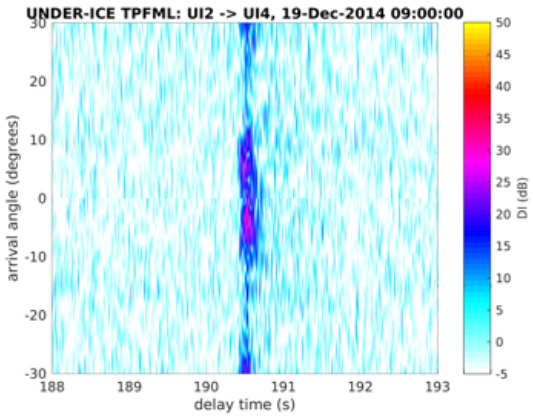

(e)

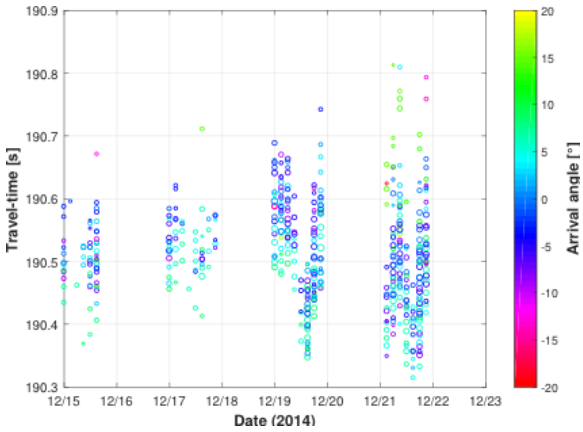

(f)

Fig. 3: Illustration of the processing chain for tomography data based on a recording at UI4 on December 19th for the transmission from UI2 at 09:00. Recorded time-domain waveform (a) and associated spectrogram (b), matched-filter output for one HM (c), matched-filter output for all HM's (d), magnitude of the beamformed signals (e), and dot-plots of arrivals in mid-December 2014 (f).

The data obtained from the UNDER-ICE experiment is described in (Storheim *et al*., 2018).

Table 1. ***Acoustic data products from UNDER-ICE project***

Dataset title	**Coverage**	**Resolution**	**Uncertainty**
Ambient noise	5 locations, 1.5 years	0-500km, 0.25days	1dB //, 20mPa / Hz
Travel time	8 sections, max. 1.5 years	100-300km, 0.25 days, major gaps	2-3 ms
Depth-range averaged ocean temperature	8 sections, max. 1.5 years	100-300km, 0.25 days, major gaps	75 mdeg

2.1.3 Acoustic data products from ACOBAR experiment

Workflow to process from hydrophone recordings to ambient noise data from the ACOBAR experiment is illustrated in Figure 3. See D2.1, Sagen et al. 2017 for more details about ACOBAR project. The recordings (0 - 500 Hz) with 100 s long are amplified, bandpass filtered, and sampled using 16-bit delta-sigma converters at a 1000 Hz rate.

Spectral density (sound pressure) for each fully scaled recording with 130 s is computed using Short-time Fourier transform (STFT) with **50 %** overlapping Hanning window and a window length of 1024 samples. The best parameters for STFT are empirically determined. 10^{th} , 50^{th} and 90^{th} percentiles of the sound pressure for every 0.9747 Hz from 0 to 500 Hz are computed. Since the sound pressure (P Pa) represents root square mean pressure, the sound pressure P is easily converted to sound level in dB by $10\ log_{10}\ P^2$. Data products provided are the median (50^{th} percentile), 10^{th} and 90^{th} percentiles which will describe the data dispersion. Similar ambient noise products will be derived for the UNDER-ICE data (see table 1) and will be important part of the analysis in WP 6.

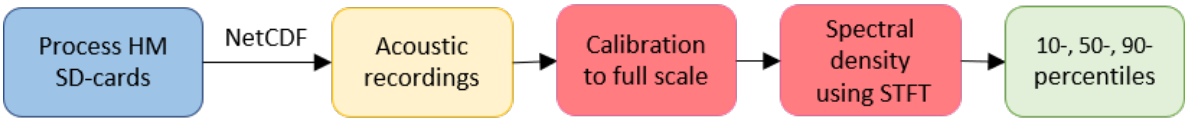

Fig. 4: Block diagram of the processing of the UNDER-ICE ambient noise data.

2.1.4. Standardization of data formats for acoustic data

Two data formats, for depth-range averaged temperature (*WTMP*) and for ambient noise (*ambientnoise*), were developed (Yamakawa et al.,2018) for the ACOBAR data presented in Sagen et al., 2017; Dushaw, 2018. The data formats were developed based on NetCDF to be easy to use for all acoustic data users and included all required information (metadata) for the

data use and further analyses. The metadata are compliant with the CF-1.6 metadata convention and OceanSITES Manual-1.2 [CF convention] (OceanSITES, 2010). More detailed description of the metadata for *WTMP* or *ambientnoise* data are given in (Yamakawa, et al. 2018).

The data format for *WTMP* was developed based on NetCDF3 architecture. *Global metadata* (general and common information for the data), *Dimensions* (dimensions of the data array) and *Variables* (data variables) are directly located in the data format (Figure 5). *Variables* consists of five variables, depth-range averaged temperature (*mean_t*), smoothed averaged temperature (*mean_t_smooth*), quality (*Z-value*) of mean_t (*mean_t_qlty*), quality flag of mean_t (*mean_t_qc*) and mean sound speed (*mean_c*). Each variable has metadata for particular to the variable and a data array. All data arrays have a common time dimension.

NetCDF4 architecture was applied to the *soundscape* data format. Metadata for *soundscape* data compliant with IOOS Convention for Passive Acoustic Recording-1.0 [Guan, et al., 2014] as well as the CF-1.6 metadata convention and OceanSITES Manual-1.2. *Global metadata*, *Dimensions* and *four Groups* are directly under the data format. Each group corresponds to a hydrophone in the DSTAR and has *Group metadata* (information for particular to the hydrophone) and *Variables*. *Variables* includes two variables, sound pressure (*sp*) and quality flag of *sp* (*sp_qc*). The two variables consist of *variable metadata* for particular to the variable and a data array. *sp* data array is a 3D matrix with time, frequency and percentiles axes and *sp_qc* data array is a vector with common time axis to the *sp* data array.

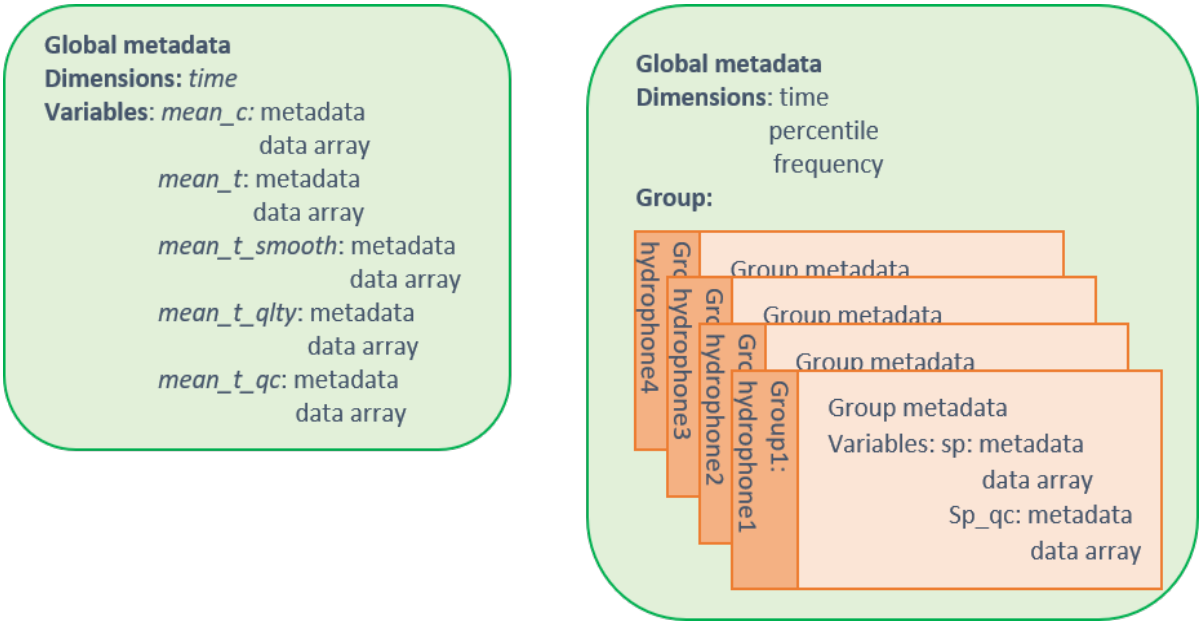

Figure 5: Structures of data formats for depth-range averaged temperature incl. acoustic travel time (left) and ambient noise (right).

Next steps in INTAROS will be to refine and employ the new data formats for UNDER-ICE data (see table 1). Furthermore, data format holding travel time data will be developed.

References

CF convention. http://cfconventions.org/

Dushaw, B. (2018). Estimating temperature in Fram Strait using DAMOCLES and ACOBAR acoustic tomography data by exploiting small-scale variability, NERSC Technical Report No.378 Version 1.0, 13 December 2017.

Dushaw B. D. and Sagen, H. "The role of simulated small-scale ocean variability in inverse computations for ocean acoustic tomography," *J. Acoust. Soc. Am.*, **142**(6), pp. 3541–3552 (2017).

Dzieciuch, M. A. "Signal processing and tracking of arrivals in ocean acoustic tomography.," *J. Acoust. Soc. Am.*, **136**(5), pp. 2512–22, (2014).

Guan, S., Moustahfid, S., Milan, A., Mize, J. (2014). A Metadata Convention for Passive Acoustic Recordings, US Integrated Ocean Observing System, Silver Spring, MD, 47 (1.0), DOI:10.13140/RG.2.1.3171.2805

Sagen, H., *et al.*, "Resolution, identification, and stability of broadband acoustic arrivals in Fram Strait," *J. Acoust. Soc. Am.*, **141**(3), pp. 2055–2068, (2017).

Storheim, E., Sagen, H., Falck, E. and Beszczynska-Möller, A. (2018). "UNDER-ICE data report", NERSC Technical Report No. 390 Version 1.0.

Yamakawa, A., Dushaw, B., Sagen, H. and T. Hamre (2018). Data standardization for long-term underwater acoustic observation - Ocean temperature and ambient noise data in Fram Strait, NERSC Technical Report No. 391, Version 1.0, 31 May 2018.

2.2 UiB and GEUS: Earthquake and focal mechanism catalog of the Arctic

An earthquake catalog is developed for the Arctic region, including new focal mechanism solutions for the larger events. The catalog covers the area north of the Arctic Circle (65.563N) and include events with magnitude 3.5 or larger in the 50-year period 196501 – 201412 (2014 is the last full year reviewed by the ISC). A complete and homogeneous earthquake catalog is a prerequisite for studying seismic hazard and temporal variation in seismicity. The derived catalog will in this regard serve as a baseline for studying changes in seismicity rates associated with long-term climatic changes.

The earthquake catalog will mainly be based on data from land stations, but will also include data from ocean bottom seismometers (OBS) as described in Deliverables D2.1 and D2.7. As the earthquakes occur in the solid earth, the detailed description of the catalog is included in Deliverable D2.8.

2.3 AWI

2.3.1 UDASH - Unified Database for Arctic and Subarctic Hydrography

Data contribution to INTAROS: temperature, salinity.

UDASH is a comprehensive, up-to-date high-quality data set of Arctic Ocean temperature and salinity north of 65°N for the period 1980–2015. The archive aims at including all publicly available data and so far consists of 288 532 oceanographic profiles (Fig. 6), formed by approximately 74 million single measurements. It includes measurements from 20 different sources, seven different platform types (ships, submarines, drifting ice camps, profiling floats, ice-tethered platforms, aircraft and one coastal station) and seven different instrument types (CTDs, expendable CTDs, STDs, bottles and digital / expendable / mechanical thermographs).

The final archive provides a unique and simple way of accessing most of the available temperature and salinity data for the Arctic Ocean [*Behrendt et al*., 2017].

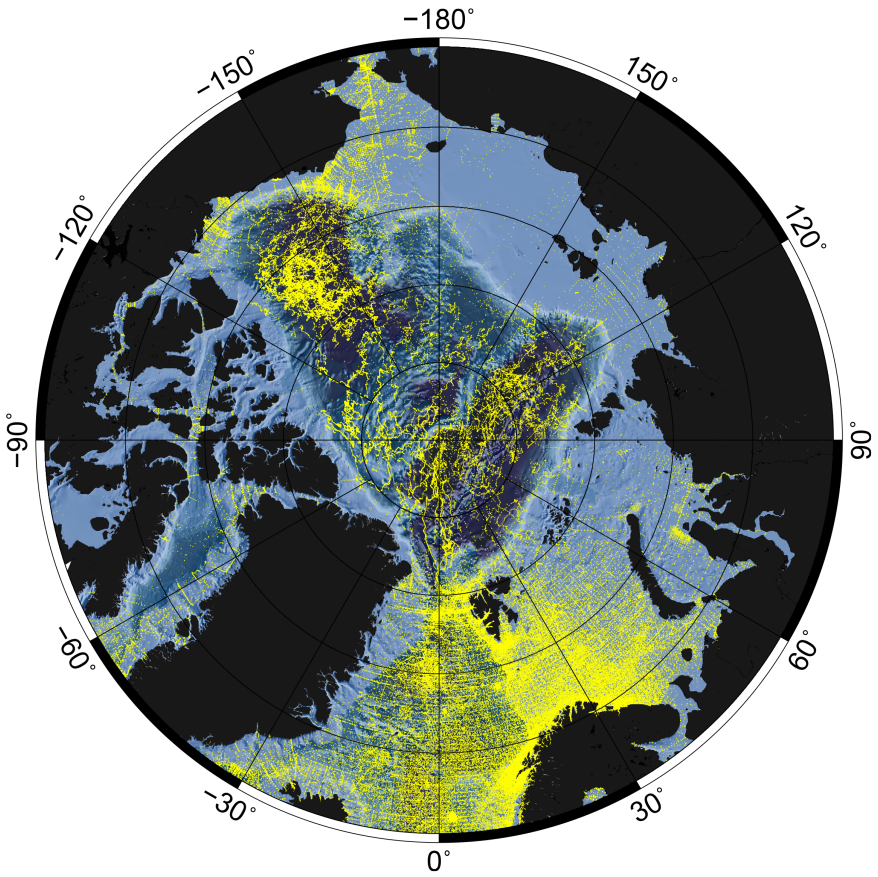

Figure 6: The distribution of UDASH profiles in the period 1980-2015.

The archive is available from the PANGAEA repository and will be updated every year. UDASH was established, as many Arctic data from the largest ocean data archive – the World Ocean Database (WOD) – were found to have a low quality. Furthermore, although WOD aims at including all data, it is lacking important data (e.g. from RV Polarstern) and therefore has significant gaps in the Arctic. Another problem is that measured ocean data sometimes do not immediately enter WOD. It may take several years for data to become available. However, WOD remains the most important source for ocean data. Approximately 75% of UDASH consist of quality-improved WOD data. To date (March 2017), UDASH contains about 15 000 profiles, which are so far not part of WOD.

Data exploitation:
All profiles that were included into UDASH have undergone very detailed quality-checking (QC) routines [details in: *Behrendt et al*., 2017]. The QC procedures include the following main steps:

1. Duplication checks
2. Position/cruise track checks
3. Gradient/outlier checks
4. Statistical screening.

Data errors or suspicious data were flagged for quick identification. Compared to WOD, the data quality increased significantly (Fig. 7).

Data in PANGAEA**:** https://doi.pangaea.de/10.1594/PANGAEA.872931

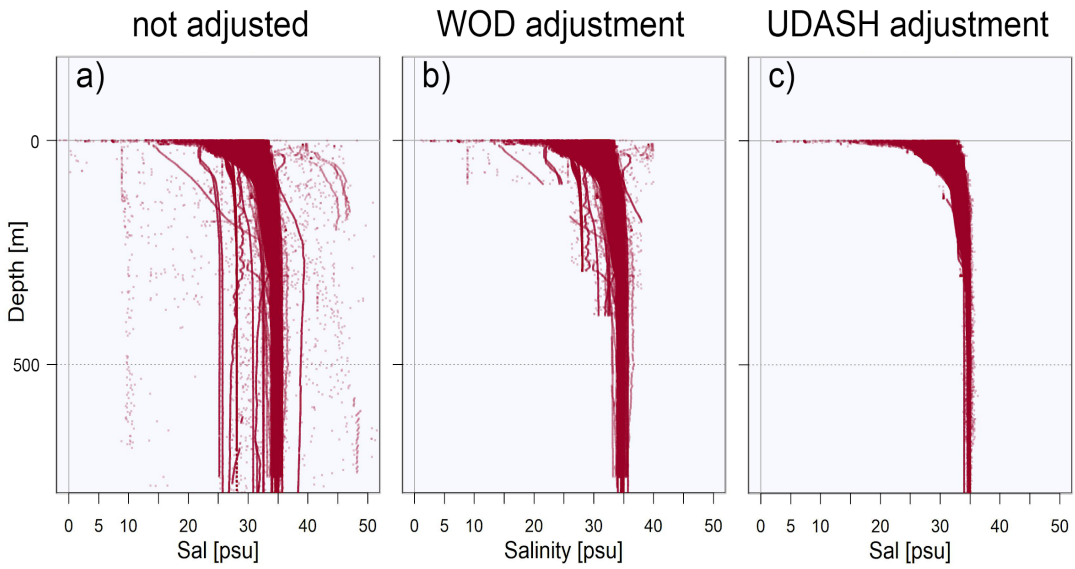

Figure 7: WOD salinity data in the Amerasian Basin. a) Data without correction. b) Accepted data according to the WOD quality flags. c) Accepted data according to the UDASH quality flags [source: Behrendt et al., 2017].

References

Behrendt, A., Sumata, H., Rabe, B., and Schauer, U.: UDASH – Unified Database for Arctic and Subarctic Hydrography, Earth Syst. Sci. Data Discuss., https://doi.org/10.5194/essd-2017-92, in review, 2017.

2.4 IOPAN

2.4.1 AREX data collection in the Nordic Seas and Fram Strait

AREX data collection includes hydrographic measurements in the Norwegian, Greenland and Barents seas, and Fram Strait gathered since 1988 during annually repeated summer (June-July) surveys of RV Oceania under the IOPAN long-term monitoring programme AREX. AREX observing system has been described in D.2.1. The long-term measurements, collected under the observational program AREX every year in the same way, provide time series of key ocean variables which allow monitoring changes of the Arctic environment and improving numerical simulations of ocean, sea ice and climate in the Arctic region. Multidisciplinary measurements include observations of the physical environment (ocean and atmosphere) and the Arctic marine ecosystem (plankton and benthos). Most of regularly repeated stations are distributed along several zonal sections, crossing the continental shelf break at the right angle and extending towards the deep basin. The zonal sections following the Atlantic water inflow from the Norwegian Sea to the northern Fram Strait allow to assess transformation of water masses originating from the North Atlantic and advected northward. Meridional sections between the

northern Norway, the Bear Island and Sørkapp, cover the eastward flow of Atlantic water into the Barents Sea.

The typical AREX hydrographic survey consists of 11-12 zonal (or in the northern part also meridional) sections extending from the outer shelf across the slope into the deep basin and two meridional sections across the Barents Sea Opening and Storfjorden trough to assess the exchange with the Barents Sea. During each survey from 120 (in early years) to 280 (in the recent decade) stations are occupied with CTD and LADCP measurements in the entire water column while underway between the station ocean currents are measured with VMADCP in the upper layer of approx. 250 m.

All hydrographic data under AREX were reprocessed to provide a unified data collection, covering the years 1988-2017 and using NetCDF3 data architecture that also includes metadata for each station. The metadata are compliant with the CF-1.6 metadata convention and OceanSITES Manual-1.2 (CF convention). The standard measured variables include temperature, conductivity and pressure of sea water. Since 2005, temperature and conductivity have been measured with a double set of sensors (two sets of data). Since 2008 chlorophyll fluorescence and since 2009 dissolved oxygen have been also measured by the CTD SeaBird system. Salinity is calculated from sea water conductivity, temperature and pressure according to TEOS-10.

Processing of CTD data included several steps and was done with the SeaBird Data Processing software and using the dedicated Matlab routines, developed by IOPAN. The standard processing protocol covers following steps:

- conversion of raw data to engineering units;
- selection and marking wild points in raw (24 Hz) converted data;
- aligning parameter data in time relative to pressure;
- low-pass filtering to smooth high frequency changes in data;
- deriving salinity from measured conductivity;
- manual cutoff of start and end of a profile (pump not working or system out of water) and visual control and manual despiking of 24 Hz temperature and conductivity data;
- removing conductivity cell thermal mass effects from the measured conductivity;
- removing pressure reversals and loops;
- averaging of all measured parameters in 1 dbar bins;
- splitting downcast and upcast in a data profile;
- calculating the derived parameters (potential temperature, potential density);
- conversion from binary to ascii data;
- conversion of profiles with averaged 1 dbar data into NetCDF format and adding metadata for each cast.

The control plots are produced for the undespiked 24 Hz data, the despiked 24 Hz data and the 1dbar-bin averaged datasets. Post cruise calibration is based on manufacturer calibration of sensors and collected water samples measured in a lab includes the 24Hz and the 1dbar-bin averaged data. Each data set represents one AREX summer survey. The processing steps are shown in Fig. 8

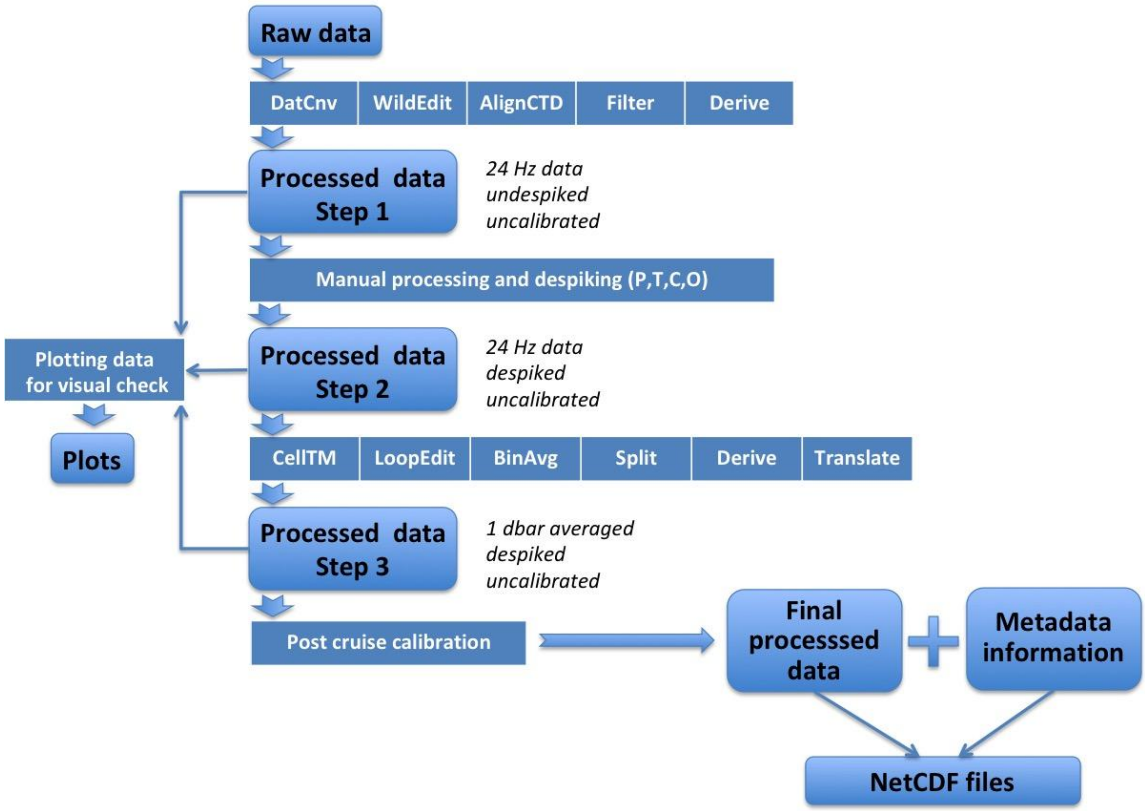

Figure 8. Schematics of AREX data processing flow

Further data exploitation included calculating of derived ocean variables based on processed CTD data sets. Following derived properties were calculated for each profile: specific volume anomaly, dynamic height, stability, and heat content. Baroclinic geostrophic currents were computed for pairs of stations and baroclinic geostrophic and total volume and heat transports across the sections were calculated. Mean properties and other statistics of Atlantic water at sections and in the selected regions were also obtained. Time series of selected derived variables were compiled for analysis of interannual variability of Atlantic water properties, transformations and transports (Fig 9).

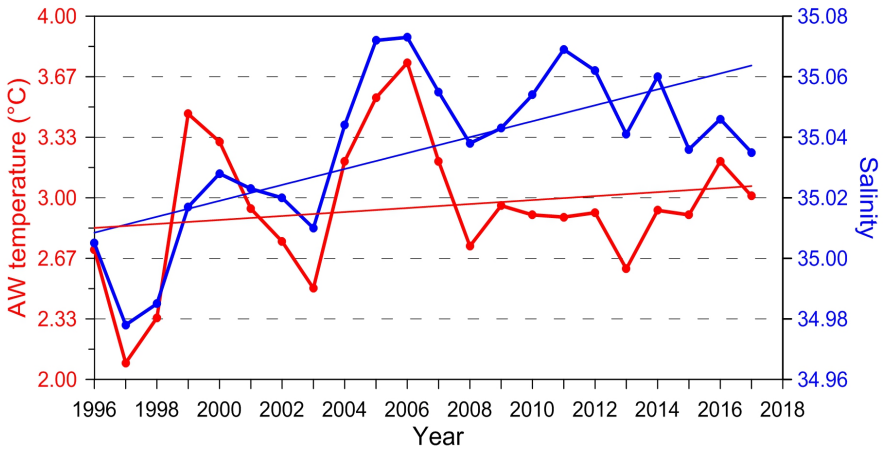

Figure 9. Example of time series of derived properties (mean temperature and mean salinity of Atlantic water) on the standard AREX section N along 76°30'E in 1996-2017.

References

Walczowski W., A. Beszczynska-Möller, P. Wieczorek, M. Merchel, A. Grynczel (2017). Oceanographic observations in the Nordic Sea and Fram Strait in 2016 under the IO PAN long-term monitoring program AREX. Oceanologia, 59(2), doi: 10.1016/j.oceano.2016.12.003

2.4.2 Processed data set from A-TWAIN Poland moorings north of Svalbard

IOPAN moorings were deployed in 2012-2013, 2013-2015 and 2015-2017 north of Svalbard as Polish contribution to the Long-term variability and trends in the Atlantic Water inflow region (A-TWAIN) project. IOPAN moorings were located over the upper slope, aiming to cover inflow both from the Svalbard and Yermak Pass Branches. One of the IOPAN moorings is usually a part of the main A-TWAIN array at 32°E while in some years the second IOPAN mooring was deployed upstream at 18 or 22°E to monitor Atlantic water transformation along the northern Svalbard slope. Under INTAROS the IOPAN moorings were augmented with new instruments measuring the profiles of ocean currents and sea ice drift and draft. Data collections from IOPAN moorings north of Svalbard are described in the relevant Questionnaires B and deliverable D2.1. In the deliverable D.2.2 we describe the processing chain and harmonisation of data formats for temperature and salinity time series collected with McLane Moored Profilers, deployed on A-TWAIN Poland moorings. The workflow for processing ocean current time series, collected with Acoustic Doppler Current Profilers (ADCP) is also described.

Each A-TWAIN Poland mooring was equipped with McLane Moored Profiler (MMP), carrying Seabird 52MP CTD sensor and Falmouth Scientific ACM Current Meter. MMP was set up to provide two profiles per day, covering the water column usually between 50 and 750-800 m depth. The MMP acquires data at a speed of 25 cm/s (with 1 Hz sampling rate) along one-way profiles separated in time by 12 h intervals. The processed data are interpolated to a 2 m fixed vertical grid. The MMP data are digitally archived in three formats and the data are identical regardless of the format. The first format stores all of the processed data from all profiles from a single MMP into single Matlab-format files. Each file contains the following variables: DPDT (array of profiling speeds cm/s), S (salinity), SIGTH (potential density sigma-theta), T (temperature), THETA (potential temperature), TIME (time of each measurement in Matlab format), U (east velocity), V (north velocity), W (measured vertical velocity that includes profiling velocity), dates (vector string with profiler start date), location (string with location of mooring), name (dataset name), number (vector of profile number), and pgrid (vector of pressure grid).

The individual ASCII profile data files are named ATWAIN_yyyy_SN_mmp###.mat, where yyyy identifies the mooring deployment period, SN is the MMP serial number and and ### is the profile number. Each individual data files includes two lines of header information. The first line provides general information (project and mooring name: profile number, start date and time, location) and the second line describes the columns of data (hr:min:sec P(Dbar) T(degC) S(PSU) U(cm/s) V(cm/s) W(cm/s) DPDT(cm/s)). The remaining lines comprise the processed data from the profile. The lines of data increase sequentially based on the time of the observation, so downgoing profiles start at the shallowest depth and upgoing profiles start at the deepest depth. Grid points with no data (that were filled with NANs) are omitted in the ASCII files.

The workflow for MMP data processing follows the procedure, described in the technical manual ‘McLane Moored Profiler Data Reduction and Processing Procedures’ by Toole (2006). The details of the procedure for downloading, processing, and archiving the MMP data include following steps:

- Retrieving MMP binary data files.
- Unpacking binary data to ASCII.
- Converting ASCII data to raw Matlab format files.
- Determining ACM heading angle and adjusting velocity biases.
- Pre-filtering, applying CTD and ACM corrections, and gridding.
- Removing spurious temperatures and salinities and adjusting to fixed reference layer.
- Interpolating to pressure grid and correcting velocities for sound speed.
- Archiving data in several formats.

Calibrations steps require additional input from laboratory CTD sensor (or SBE37 sensor deployed on the same mooring and pre- and post-deployment CTD casts) and ACM compass calibration information. This is used to determine and apply Velocity bias corrections and to calibrate and quality control the CTD conductivity data.

As the top of the MMP measurements is located between 50-100 m, they sample the water column below the surface mixed layer. Two additional CTD sensors (SBE37) located above and below MMP depth range provide data to calibrate the MMP CTD sensor (SBE52) and extend the measurement range by additional 2-3 m below and above MMP profile. SBE37 raw time series of temperature, conductivity and pressure are processed according to the standard procedure that includes data conversion, despiking and averaging onto 1 hour interval. For comparison and merging with temperature and salinity from MMP profiles, SBE37 data are subsampled to the MMP interval (12 hours). The example of temperature comparison is shown on Fig. 10.

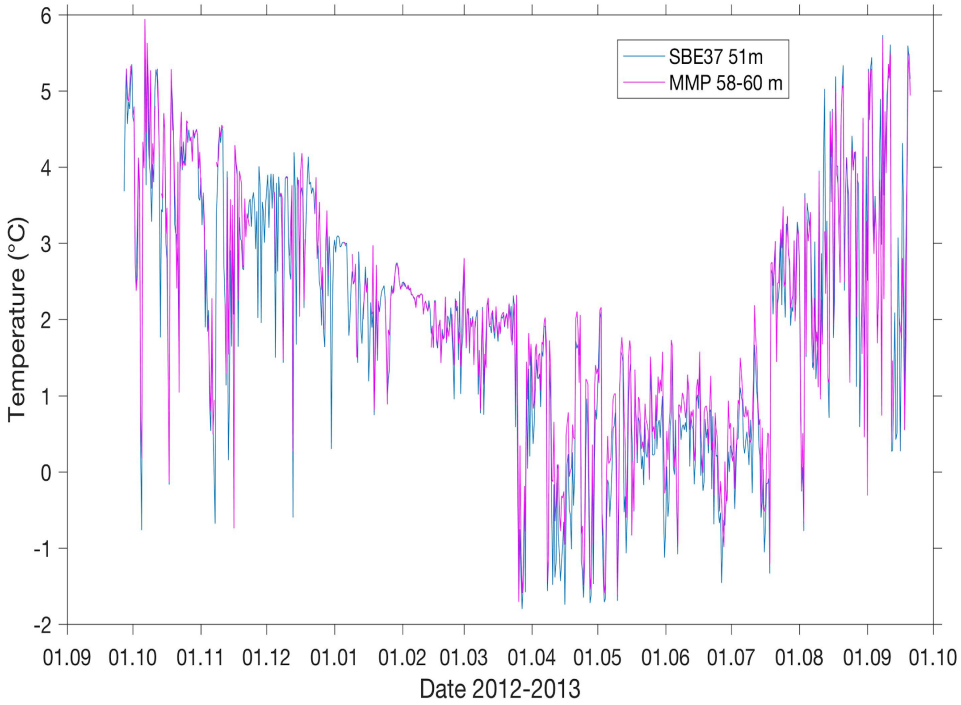

Figure 10. Example of comparison between temperature time series collected by SBE37 at the nominal depth of 51 m and MMP SBE52 averaged between 58-60 m at the mooring IOPAS6 in 2012-2013.

For further analysis temperature profiles from MMP and time series from SBE37 are averaged daily and merged with sea surface temperature from the NOAA High-resolution Blended Analysis of Daily SST and Ice on 0.25 deg grid (Reynolds et al., 2007). The missing data between the sea surface and the first depth of temperature measurement at a mooring are filled by linear interpolation. The example of daily temperature time series in the upper 750 m is shown on Fig. 11.

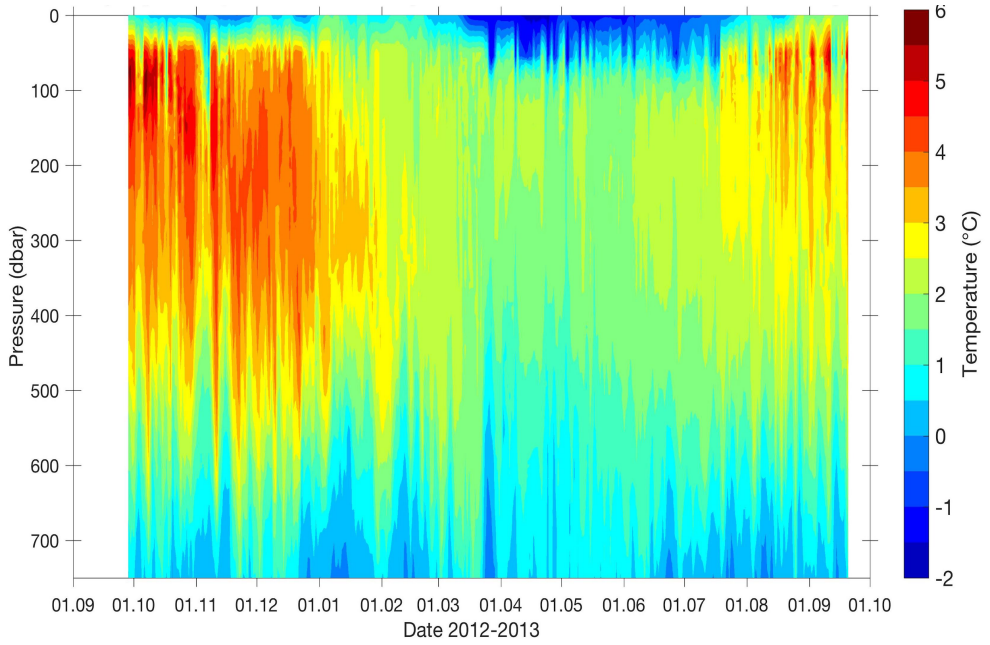

Figure 11. Example of the upper 750 m daily temperature product from merged MMP profiles, SBE37 time series and SST from OISSTv2 at the mooring IOPAS6 in 2012-2013.

Processed temperature, salinity and ocean currents data products from MMP measurements were converted into NetCDF format and the metadata compliant with the CF-1.6 metadata convention and OceanSITES Data Format Reference Manual [CF convention] (OceanSITES, 2015) were added for each file.

Processing of ADCP data from the A-TWAIN Poland mooring 2015-2017 (no ADCP in the earlier deployments) includes extraction of data from the ADCP binary files, correction for magnetic declination, quality control procedures and re-mapping on the constant depth strata. The workflow for ADCP data post-processing and quality control consists of following steps:

- Magnetic declination correction and direction test.
- In and out the water test.
- Calculating distance from the surface to the centre of each depth cell.
- Re-mapping data on uniform depth strata.
- Tilting angle test.
- Side lobe test.
- Coarse outlier removal.
- Tests of additional parameters (echo intensity, correlation magnitude, percent of good, error velocity and vertical velocity) to identify potentially bad data.

Processed ocean currents data products from ADCP measurements are converted into NetCDF format and the metadata compliant with the CF-1.6 metadata convention and OceanSITES Data Format Reference Manual [CF convention] (OceanSITES, 2015) are added for each data file.

References

OceanSITES (2015). OceanSITES Data Format Reference Manual. NetCDF Conventions and Reference Tables. Version 1.3, January 12, 2015.

Reynolds, R.W., T.M. Smith, C. Liu, D.B. Chelton, K.S. Casey, M.G.R Schlax (2007). Daily High-Resolution-Blended Analyses for Sea Surface Temperature. J. Climate, 20, 5473-5496.

2.4.3 Argo float data sets from deployments in the Nordic Seas

Argo data from the satellite operators are provided to Data Assembly Centres (DACs), decoded and quality controlled. Errors are flagged and corrected where possible. Then data are passed to the Coriolis Global Data Centre (GDAC). There are Real Time Data (RT) available for users within 24 hours after transmission. These data may still contain errors. Therefore the second, 'delayed mode' (DM) data processing and validation takes a place in Argo Regional Data Centers. These centers should provide wide expertise on specific geographical ocean regions, own large databases of shipborne observations.

Institute of Oceanology PAS provides expertise on the Arctic region observations, has own database from the AREX cruises. Therefore we started to process the Argo data collected over the ArgoPoland project to obtain and deliver Delayed Mode products. For improving the qualifications and quality of data processing, two oceanographers from IOPAS participated the Argo Data processing workshop organised by Euro-Argo RI. Additionally, to help other Argo floats DM data processing, IOPAS provides own CTD data obtained during AREX cruises to global ARGO datacenter.

2.4.4 Hydrographic data sets from long-term monitoring in Svalbard fjords

Here, we provide two comparable hydrographic data sets collected by the Institute of Oceanology PAS during Arctic cruises of RV Oceania and land-based measurement campaigns with a small boat in two Arctic fjords, Hornsund and Kongsfjorden, being the southernmost and the northernmost component of the west Spitsbergen fjords' network. Data collections were reported in six questionnaires B and described in the deliverable D2.1. The high resolution CTD sections are performed every year in Hornsund and Kongsfjorden (Fig. 12). All data were re-processed and converted to common format and stored in NetCDF files with metadata added. Sections were divided into regions (fjord mouths, central part, deep fjord) and time series of mean water properties for so divided sections were calculated. Additionally, fresh water content (FWC) was calculated by the integration of measured salinity relative to a reference salinity of 34.2 over the entire water column. To complement the standard sections by a towed system, since 2010 CTD measurements are performed from a small boat at repeated stations in the Hornsund glacial bays. All measurements were re-processed and converted to common format. The fjord observation database was established.

In summers of 2016 and 2017 the pioneering measurements of water column microstructure close to the tidewater glaciers were performed. Data were processed and interpreted. The rate of dissipation of turbulent kinetic energy in various fjord's regions was calculated. The unexpected high, rare observed rate of dissipation of turbulent kinetic energy were observed in plumes of subglacial discharges. The obtained results (rates of dissipation, eddy diffusivity) will be used in numerical modelling of the glacier-ocean interactions.

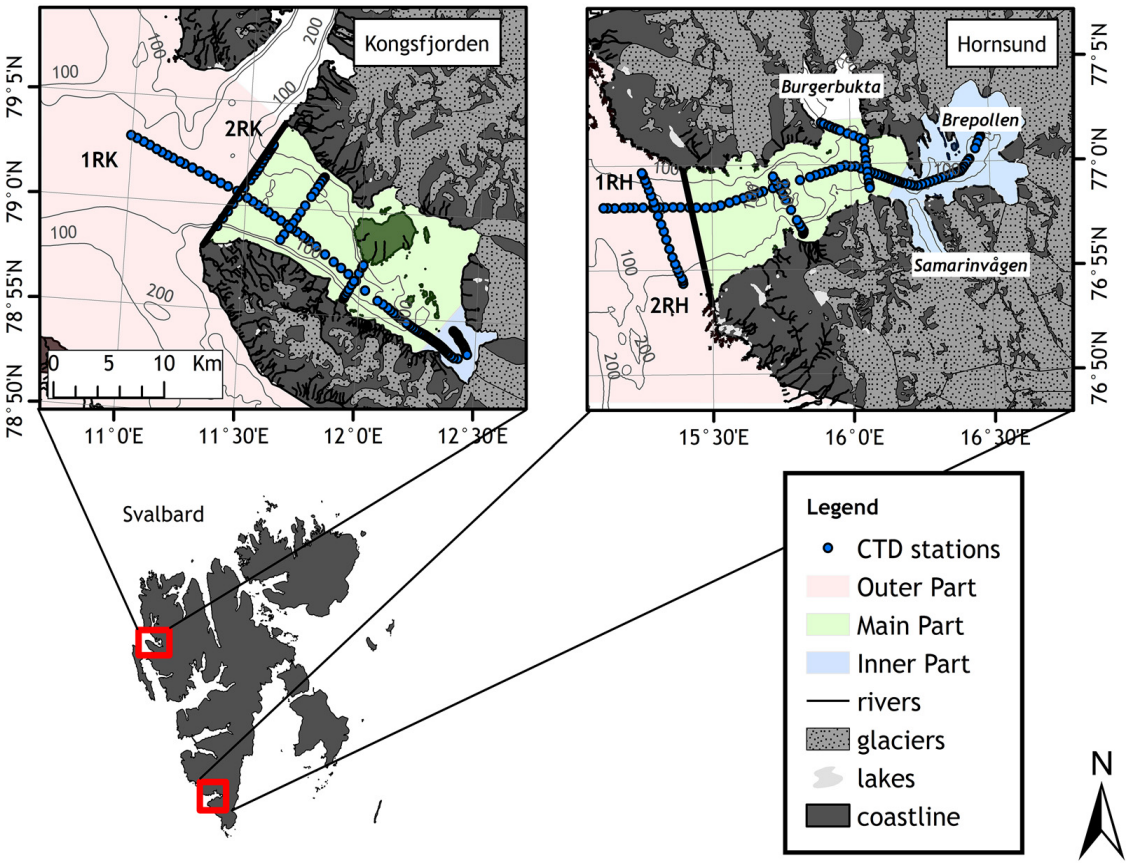

Figure 12. Location of CTD stations in Kongsfjorden and Hornsund. Black lines indicate geographical boundaries of the fjords. Different colors represent different parts of the fjords: Outer part (light coral), Main part (light green), Inner part (light blue) (from Prominska et al. , 2017).

References

Promińska A., M. Cisek, W. Walczowski, (2017), Kongsfjorden and Hornsund hydrography — comparative study based on a multiyear survey in fjords of west Spitsbergen, Oceanologia 59, 397—412

2.5 DTU Space

In Deliverable 2.1 the existing satellite altimetry dataset is assessed. The dataset includes data from 1991-2017. In this report different exploitations of the altimeter data is described.

2.5.1 Sea Level Anomaly

Different reprocessing methods are used to process the sea level anomaly that is tailored for the Arctic region. For ERS-1, ERS-2 and Envisat (from 1991-2012) the retracking method by the RADS-database is used with the addition of allowing for low significant wave heights (SWH), which quadruples the amount of data some regions. For the Cryosat-2 data (2011-2017), which covers up to 88° N, a DTU-developed retracking system is used. The satellite tracks are gridded in monthly 0.5x0.5 degree grids, covering from 68°N-82°N/88°N. Figure 13 shows the trend from 1991-2017.

Medio/Ultimo 2018 will Sentinel-3 data be included in the Sea Level Anomaly product.

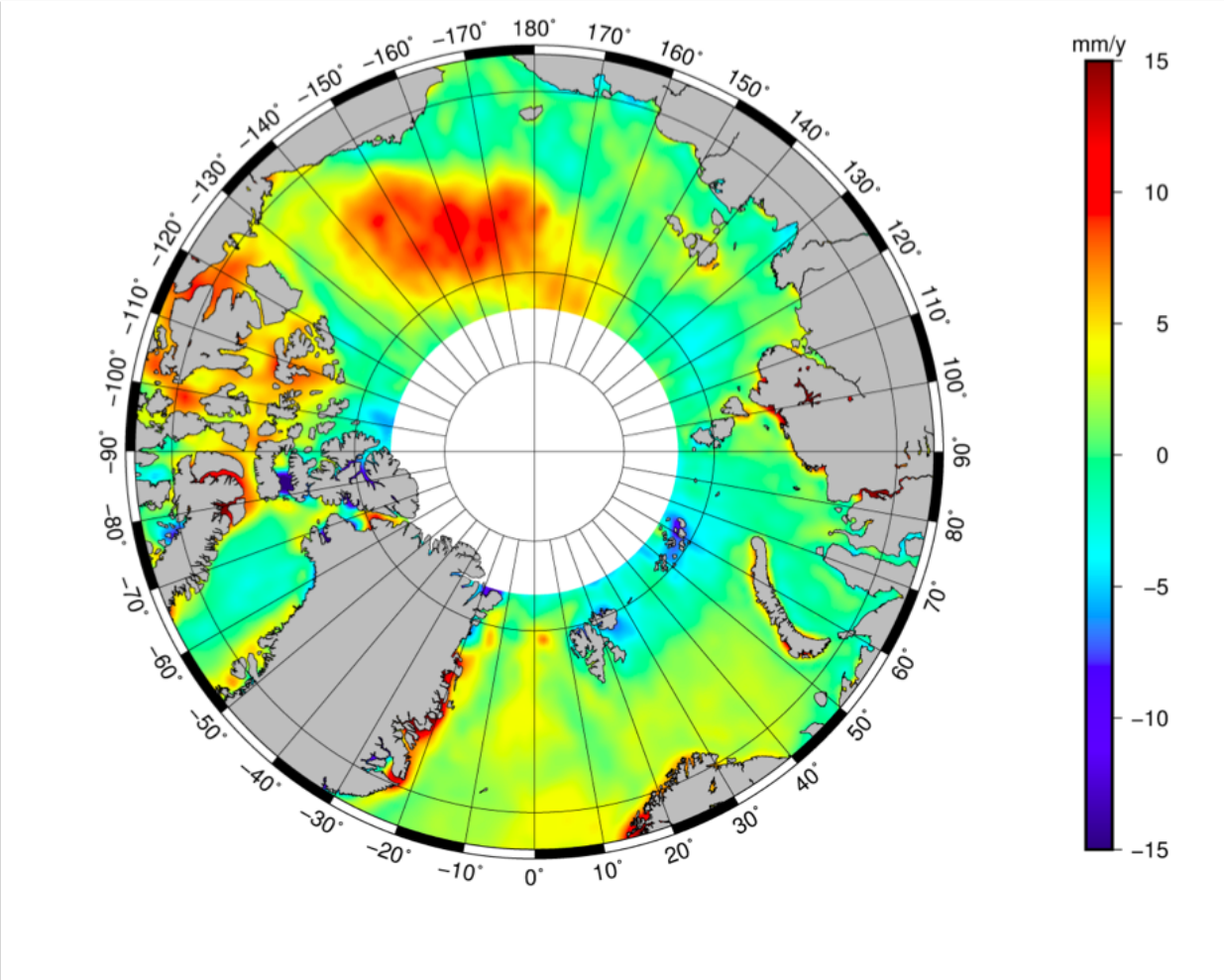

Figure 13. Sea level anomaly trend from 1991-2017 i mm per year. It covers data from ERS-1/ERS-2, EnviSat and CryoSat-2. The data processing is tailored to the Arctic before gridding to a 0.5° x 0.5° monthly grid.

2.5.2 Mean Sea Surface

From the 26 years of altimetry data, DTU has created a sea level reference surface, the Mean Sea Surface (MSS). The latest version DTU15MSS uses a reference for the Sentinel-3 mission. It includes CryoSat-2 up to 88°N and uses Synthetic Aperture Radar (SAR)-mode which improves coverage in coastal and archipelago regions. Example of MSS is shown in Fig. 14.

2.5.3 Mean Dynamic Topography

The mean dynamic topography (MDT) is the difference between the geoid and the mean sea surface. The MDT can be used to reveal currents and permanent temperature variations. The geoid model used is the Eigen-6C (Förste et al, 2011). Example is shown in Fig. 15.

The data products are available in ascii and grid format at the DTU Space server: ftp://ftp.space.dtu.dk/pub/ARCTIC_SEALEVEL

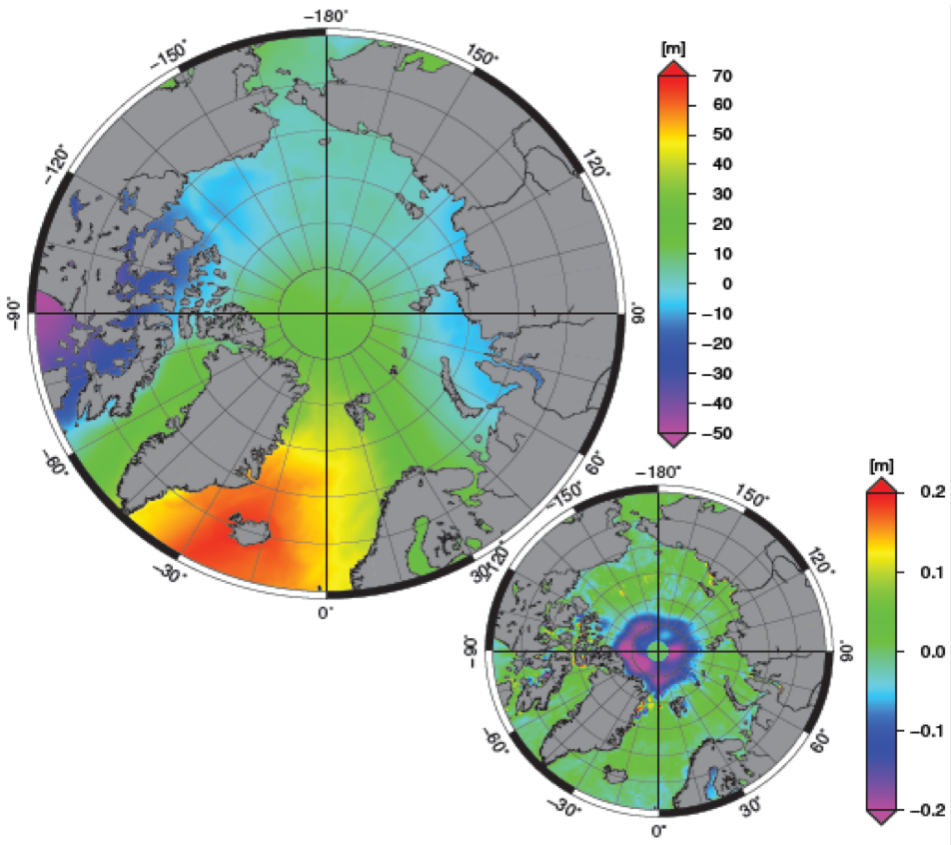

Figure 14. The large plot shows DTU15MSS relative to the earth ellipsoid. The small plot to the right shows the difference between DTU13MSS and DTU15MSS. It clearly reflects the updated data between 82° and 88° N

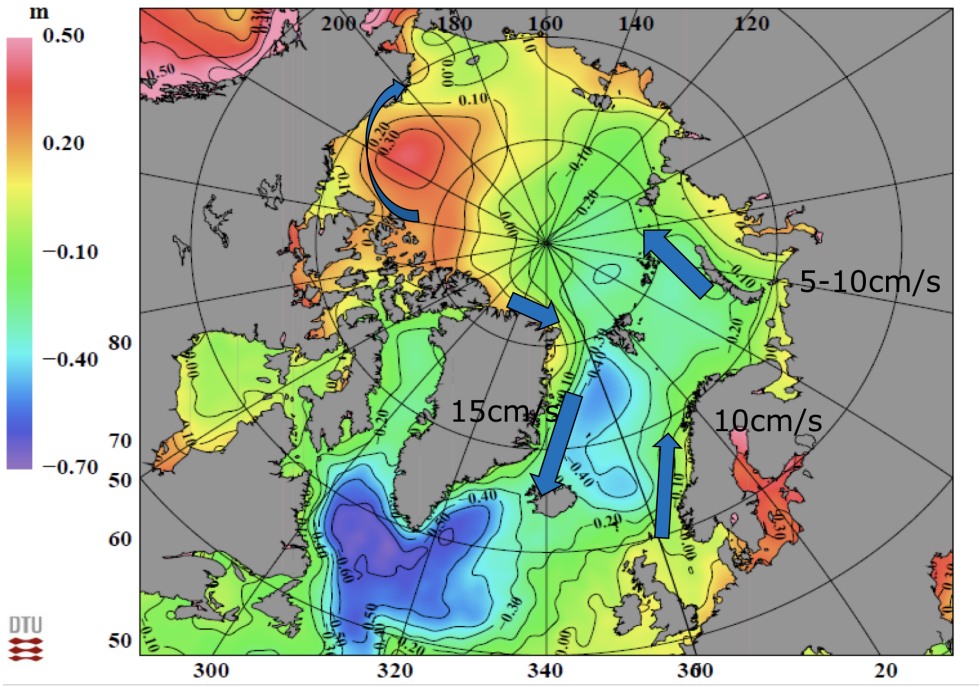

Figure 15. Mean Dynamic Topography (difference between DTU15MSS and Eigen-6C). The main currents are highlighted by blue arrows and the speed has been calculated (colour bar).

References

Andersen, O. B., & Piccioni, G. (2016). Recent Arctic Sea Level Variations from Satellites. Frontiers in Marine Science, 3, [76]. DOI: 10.3389/fmars.2016.00076

Cheng, Y., Andersen, O. B., and Knudsen, P. (2015). An improved 20-year Arctic Ocean altimetric sea level data record. *Mar. Geod.* 38, 146–162. doi: 10.1080/01490419.2014.954087

Passaro, M, P. Cipollini, S. Vignudelli, G. D. Quartly. H. M. Snaith (2014) "ALES: a multi-mission adaptive sub-waveform retracker for coastal and open ocean altimetry", Rem. Sens. Environ., V. 145, pp. 173–189, http://dx.doi.org/10.1016/j.rse.2014.02.008.

Rose, S. K., Andersen, O. B., Passaro, M, P., Benvieste, J. (2017) "An updated 25+ year (1991-2017) sea level record from the Arctic Ocean", EGU presentation, Vienna.

Scharroo, R., Leuliette, E. W., Lillibridge, J. L., Byrne, D., Naeije, M. C., and Mitchum, G. T. (2013). "RADS: Consistent multi-mission products," in *Proceedings of the Symposium on 20 Years of Progress in Radar Altimetry,* (Venice: Eur. Space Agency Spec. Publ., ESA SP-710), 4.

Stenseng, L. (2011). *Polar Remote Sensing by CryoSat-type Radar Altimetry*. Ph.D. thesis. National Space Institute, Technical University of Denmark.

2.6 Aarhus University

The Greenland Ecosystem Monitoring Programme collects an extensive range of physical, chemical and biological variables which allow both the quantification of climate change but also an analysis of the potential biological consequences in both terrestrial, limnic and marine systems. The programme is centered around two key sampling sites in Greenland; sub-arctic Nuuk in West Greenland and high-Arctic Zackenberg in East Greenland. The key objective of the programme is to provide standardized time series of quality checked data for the scientific community. Therefor all data are made available on the GEM database. An outline of findings and trends in the program is also presented as annual "report cards" (http://g-e-m.dk/news/nyhed/artikel/gem-annual-report-cards-2016-first-edition/). For the physical ocean data (described in D2.1) obtained from either repeated ctd transects or moorings are checked by: 1) Plotted in GIS software to confirm positions 2) standardized check for outliers.

One important task for Arctic marine research is to quantify how changes in the Arctic cryosphere influence the freshwater content of the ocean. Here, the time series from Young Sound has been used to quantify the extent of the freshening in Greenland coastal water which are influenced by melting of the Greenland Ice Sheet but also melting sea ice. Based on the repeated CTD transect in Young Sound, East Greenland, data from 2003 to 2015 were used to show inter-annual changes in salinity for different sections of the fjord. A significant decrease in salinity was found in the fjord, with evidence that this freshening was driven by lower salinity of the coastal water (Sejr et al. 2017). The analysis was extended based on the continuous mooring (Fig 16) which allowed us to identify 2005-2007 as the period where the most dramatic freshening took place (Boone et al. 2018).

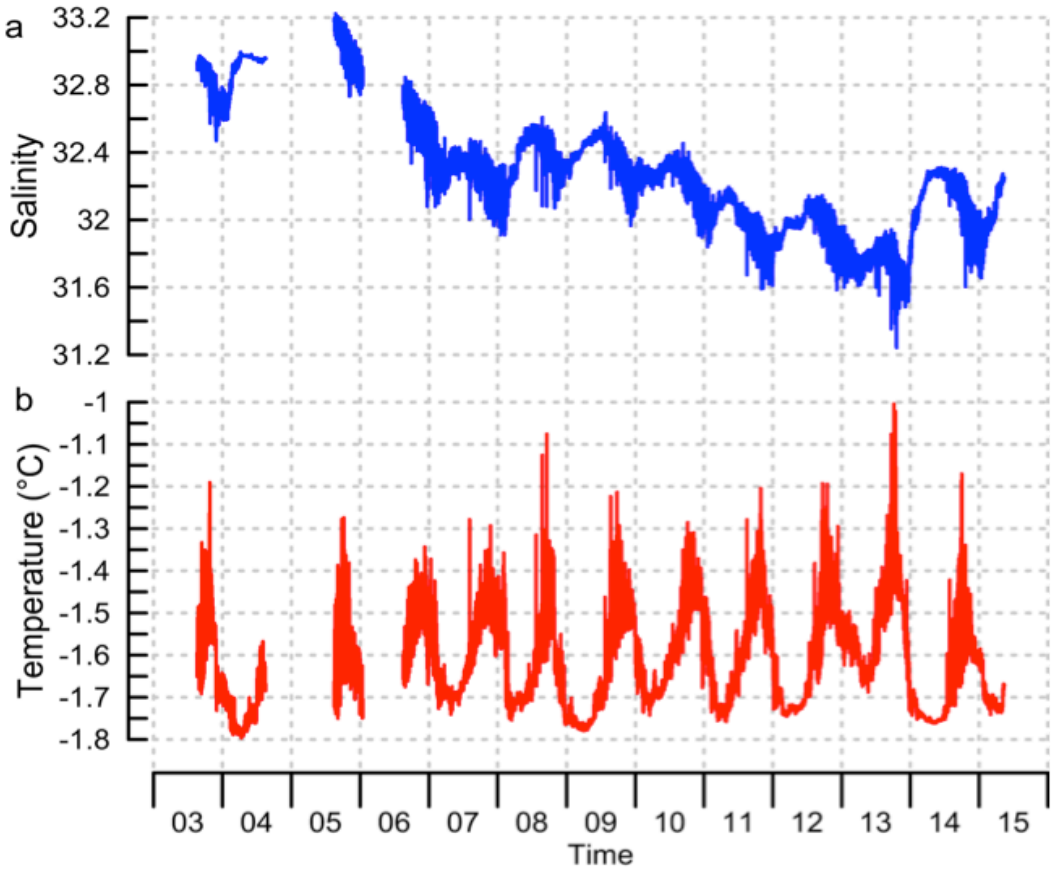

Figure 16. Temperature and salinity from 60 m depth from the Greenland Ecosystem Monitoring program in Young Sound. 2003 to 2015. Redrawn from Boone et al. 2018.

References

Wieter, Boone, et al. "Coastal freshening prevents fjord bottom water renewal in Northeast Greenland-a mooring study from 2003-2015." *Geophysical Research Letters (online)* (2018).

Sejr, Mikael K., et al. "Evidence of local and regional freshening of Northeast Greenland coastal waters." *Scientific reports* 7.1 (2017): 13183

2.7 IFREMER

2.7.1 Arctic sea ice displacement from low-resolution satellite data

Sea ice displacement can be inferred from single sensors. We proposed here an enhanced product at low resolution using both radiometer data and scatterometer data. From the individual estimate of the displacement using classical Max Cross Correlation techniques, we compute a merged product which enables higher reliability, more vectors (90% of information from October until April, less in September and May, no in summer) and longer period (September and May) compared to the individual products.

The sea ice displacement vectors are estimated at 3 and 6 day lags, using SSMI radiometer data and QuikSCAT and ASCAT scatterometer data, allowing to have 62.5 km grid resolution Arctic sea ice concentrations maps daily since 1992.

Method and validation with buoys are presented in details by Girard-Ardhuin & Ezraty (2012). Comparison with other products exist, for example in Sumata et al (2014), this product has been used in many projects and publications.

The data are processed routinely, archived and distributed by the CERSAT at Ifremer freely at friendly format and easy access (FTP). User manual is available on the portal. Example of low-resolution sea ice displacement is shown in Fig 17.

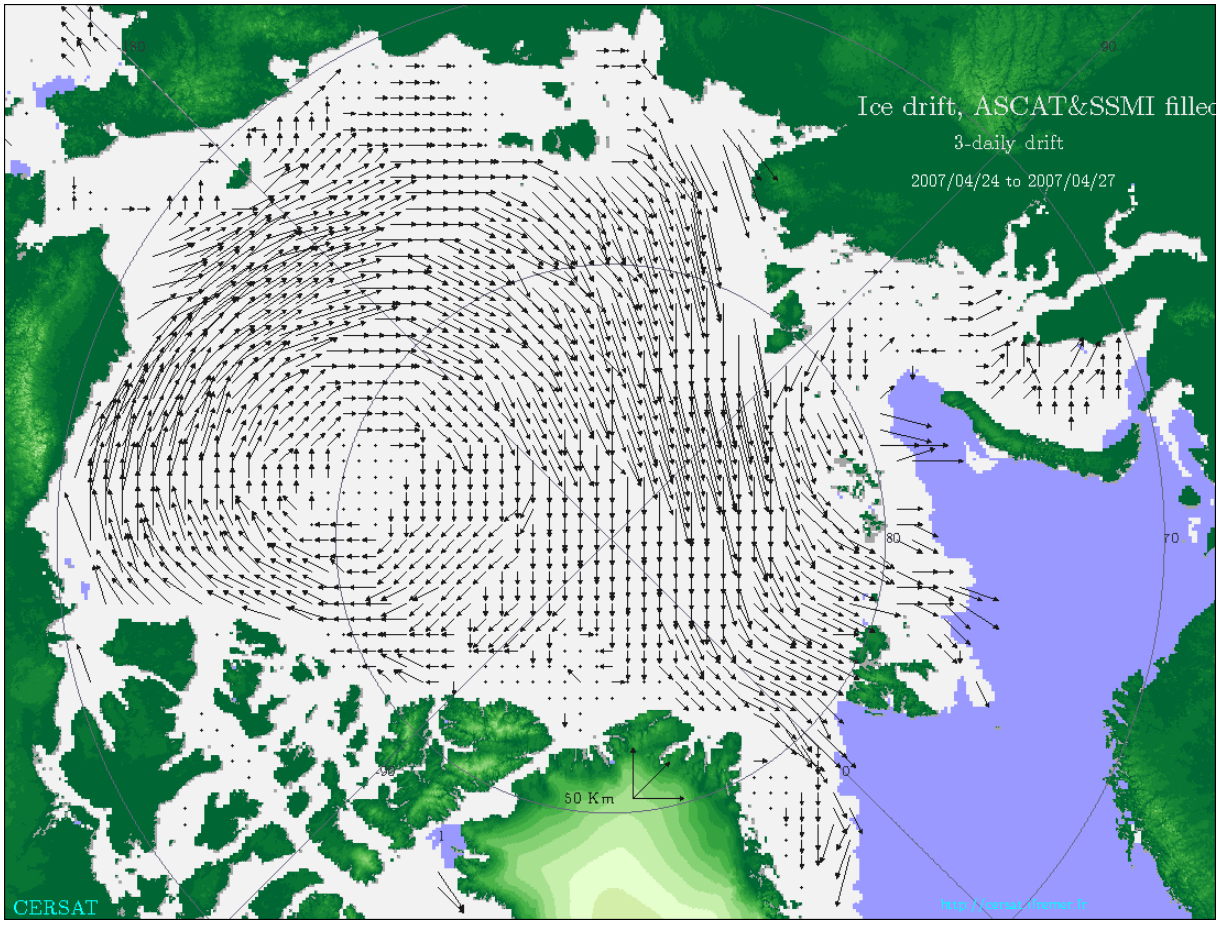

Figure 17: Arctic mean sea ice displacement at medium resolution at 3 day-lag between April 24 and 27th, 2007 at low resolution using SSMI and ASCAT/MetOp-A sensor data. More than 90% of the vectors are estimated over the sea ice area.

2.7.2 Arctic sea ice displacement at medium resolution from satellite data

(F. Ardhuin, Ifremer)

Sea ice displacement can be inferred from single sensors. We proposed here an enhanced product at medium resolution using both H and V polarisation of AMSR radiometer sensors. From the individual estimate of the displacement using classical Max Cross Correlation techniques, we compute a merged product. The sea ice displacement are estimated at 2, 3 and 6 day lags, using AMSR-E and AMSR2 radiometers data, allowing to have 31.25 km grid resolution Arctic sea ice concentrations maps daily since 2002 (gaps between the 2 sensors in 2011).

Method and validation with buoys are presented in details by Girard-Ardhuin & Ezraty (2012). Comparison with other products exist, for example in Sumata et al (2014), this product has been used in many projects and publications.

The data are processed routinely, archived and distributed by the CERSAT at Ifremer freely at friendly format and easy access (FTP). User manual is available on the portal. Example of medium resolution sea ice displacement is shown in in Fig. 18.

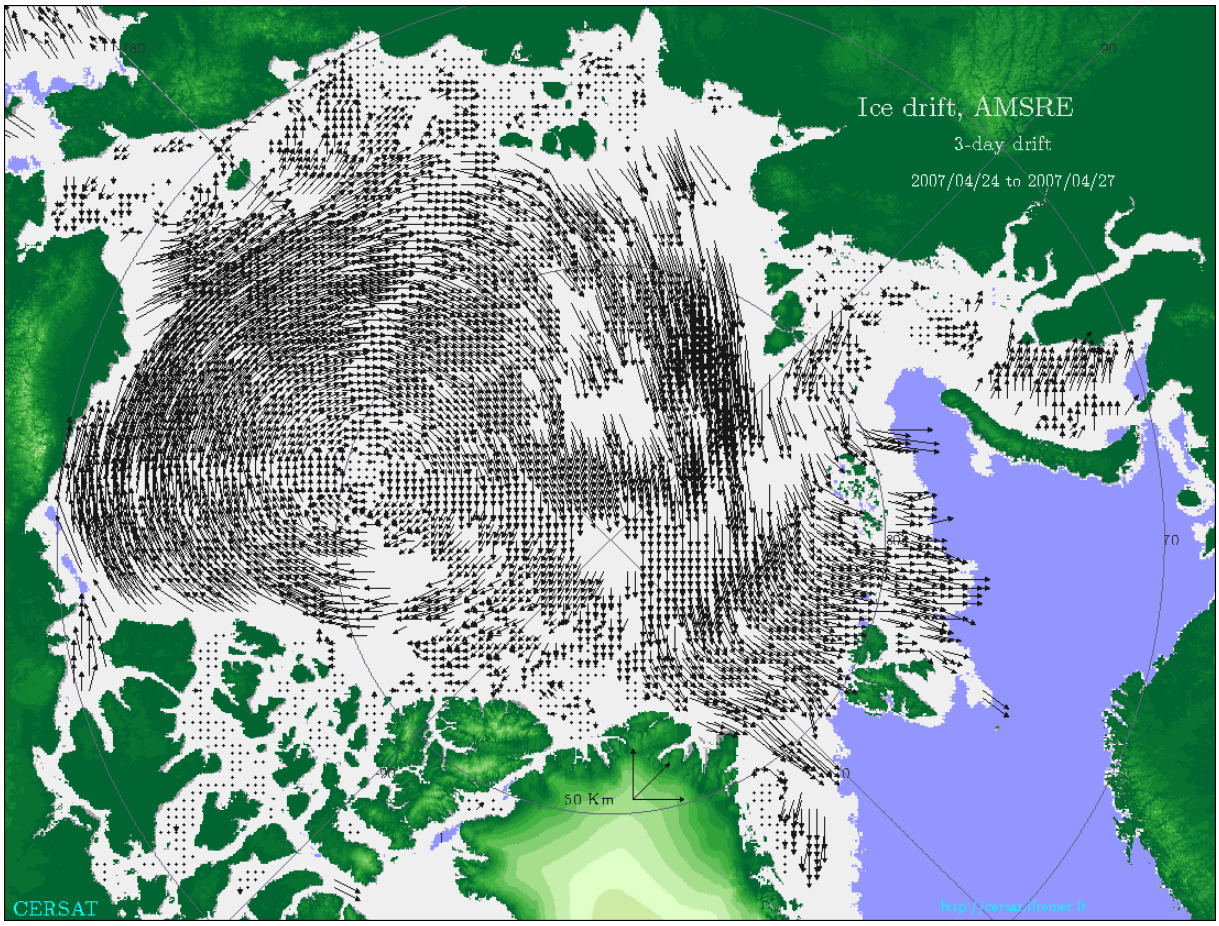

Figure 18: Arctic mean sea ice displacement at medium resolution at 3 day-lag between April 24 and 27th, 2007 at medium resolution using AMSR-E sensor channels data. Compared to the example of Fig. 17, the angular resolution is better but there are more data gap patches.

References:

Girard-Ardhuin, F., R. Ezraty, 2012 : Enhanced Arctic sea ice drift estimation merging radiometer and scatterometer data. *IEEE Trans. Geosci. Remote Sensing*, vol. 50 (7), July 2012, pp 2639-2648. Doi : 10.1109/TGRS.2012.2184124.

Sumata, H., T. Lavergne, F. Girard-Ardhuin, N. Kimura, M.A. Tschudi, F. Kauker, M. Karcher, R. Gerdes, 2014 : An intercomparison of Arctic ice drift products to deduce uncertainties estimates**.** *J. Geophys. Res. Ocean,* vol. 119, July 2014. DOI : 10.1002/2013JC009724.

2.8 University of Bremen

2.8.1 Multiyear sea ice concentration product based on AMSR2 and scatterometers

Need of product. Arctic sea ice has decreased dramatically over the last three decades. The decrease is particularly pronounced in September when the annual sea ice minimum occurs, and particularly so for the area of multiyear ice (MYI), i.e. sea ice which has survived at least one summer. MYI strongly differs from first-year ice (FYI) in physical, radiative and dynamic properties. The spatial distribution of MYI is required for climate modeling, numeric weather forecast and sea ice prediction. The MYI distribution is retrieved based on microwave satellite observations. Specific weather conditions and ice deformation can cause MYI misclassification, which is corrected using sea ice drift satellite data and temperature information from atmospheric model reanalysis.

Data Exploitation. The MYI concentration C_MY is defined as the fraction of an ocean area that is covered with MYI. C_MY is 0% over open water (ice-free ocean), and 100% over full MYI covered ocean. Over an area covered with 25% FYI and 25% MYI, C_MY would be 25%. That is, C_MY never exceeds the total sea ice concentration for which many retrieval algorithms exist.

The multiyear ice retrieval method suggested here is based on ECICE MYI retrieval algorithm (Shokr et al., 2013) plus two correction schemes discussed below. ECICE is a flexible algorithm that does not rely on single tie-points but instead uses probability distributions of the radiometric features for the different surface types (MYI, FYI, open water). For the combination AMSR-E with QuikSCAT the two polarizations of the AMSR-E 37 GHz channels, plus Seawinds/QuikSCAT 13.4 GHz (Ku-band) HH and VV scatterometers data is used (Ye et al, 2016, 2016a). Example of MY-concentration is shown in Fig. 19 (mid panel).

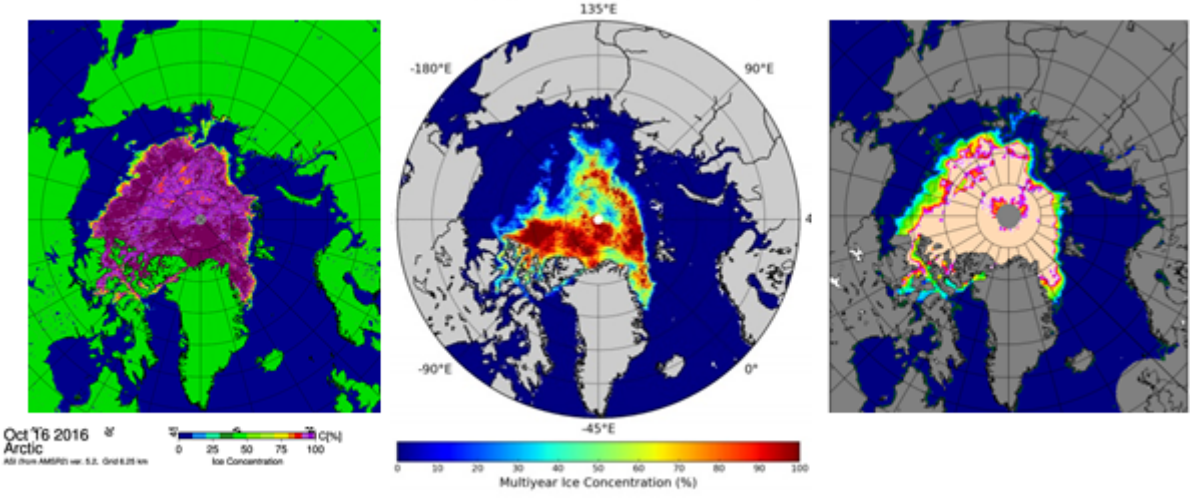

Figure 19: Sea ice concentration (left), multiyear ice concentration (middle) and thickness of thin sea ice (right) as of 16 Oct 2016. Total ice concentration is described in Deliverable 2.1 (present capabilities), multiyear ice concentration and thickness of thin sea ice Deliverable 2.2 (this document).

This method was recently adapted to AMSR2 and ASCAT data where the ASCAT 5.3 GHz VV channel is combined with AMSR2 37 and 19 GHz H and V channels. In both cases a linear combination of brightness temperature from the 18.7 GHz and 23.8 GHz channels is used to filter out open water pixels. After the retrieval two corrections are applied.

The first correction based on air temperature records restores underestimated MYI concentrations under warm (melting) conditions (Ye et al. 2016). The second correction reduces overestimated C_MY values based on sea ice drift data. These errors may be caused by sea ice deformation, snow wetness and metamorphism (Ye et al. 2016a). Note that these two correction schemes may also be combined with other multiyear ice concentration retrievals, with expected similar success.

Reliable ground truth data of multiyear ice concentration at intermediate values and on the scale of passive microwave satellite observations are difficult to obtain. Therefore, current validations are based on regions of 0% and 100% multiyear ice concentrations, and on plausibility checks (day to day changes) of time series.

Until now, the algorithm has been developed and applied for several years of historic data. Here, the algorithm is brought to operational NRT application. During the implementation process, several flaws have turned out and are adjusted.

References:

Shokr, M.; Agnew, T.A. Validation and potential applications of Environment Canada Ice Concentration Extractor (ECICE) algorithm to Arctic ice by combining AMSR-E and QuikSCAT observations. Remote Sens. Environ. **2013**, 128, 315–332.

G. Spreen, L. Kaleschke and G. Heygster 2008: Sea ice remote sensing using AMSR-E 89 GHz channels. J. Geophys. Res 113, C02S03, doi:10.1029/2005JC003384.

Ye, Y.; Heygster, G.; Shokr, M. Improving multiyear ice concentration estimates with reanalysis air temperatures. IEEE Trans. Geosci. Remote Sens. **2016**, 54, 2602–2614.

Ye, Y.; Shokr, M.; Heygster, G.; Spreen, G. Improving Multiyear Sea Ice Concentration Estimates with Sea Ice Drift. *Remote Sens*. **2016a**, *8*, 397.

2.8.2 Thickness of thin sea ice retrieval from L band satellite sensors SMOS and SMAP

Need of product. Together with sea ice concentration, sea ice thickness belongs to the most important sea ice parameter required for climate modeling, weather prediction and operational ship routing. The thickness of the ice determines its resistance against the deforming forces of wind and ocean currents. Even a thin layer of sea ice inhibits evaporation, reduces heat and gas exchange between ocean and atmosphere and increases the albedo. It provides a solid surface for snow to deposit, which further reduces heat exchange and increases albedo. The sensitivity of these physical parameters to thickness is strongest at thin sea ice. Methods to retrieve the thickness of thin sea ice from microwave satellite observations in the L band (1.4 GHz) have been suggested based on data of SMOS satellite launched 2009 (Kaleschke et al. 2012, Huntemann et al. 2014) and based on a combination with edata from the L band radiometer SMAP launched 2015 (Patilea et al., 2017).

Data Exploitation. The data product based on the combination of SMOS and SMAP data has proven to be less vulnerable to RFI contamination and more stable. In INTAROS, the combined data product will be made available operationally and in near real time.

References

Huntemann, M., Heygster, G., Kaleschke, L., Krumpen, T., Makynen, M., and Drusch, M.: Empirical sea ice thickness retrieval during the freeze-up period from SMOS high incident angle observations, The Cryosphere, 8, 439–451, 2014.

Huntemann, M., Patilea, C., and Heygster, G.: Thickness of thin sea ice retrieved from SMOS and SMAP, in: Proceedings of 2016 IEEE International Geoscience and Remote Sensing Symposium (IGARSS), pp. 5248–5251, 2016.

Kaleschke, L., Tian-Kunze, X., Maaß, N., Mäkynen, M., and Drusch, M.: Sea ice thickness retrieval from SMOS brightness temperatures during the Arctic freeze-up period, Geophysical Research Letters, 39, l05501, 2012.

C. Patilea, G. Heygster, M. Huntemann, and G. Spreen: Combined SMAP/SMOS Thin Sea Ice Thickness Retrieval. The Cryosphere Discuss., https://doi.org/10.5194/tc-2017-168. Manuscript under review for journal The Cryosphere, 2017.

2.9 NIVA

NIVA produces in situ datasets for Arctic carbonate system chemistry, nutrients, and phytoplankton biomass. For INTAROS we contribute with: 1) surveyed existing data collections, and 2) analysed the data collections for data coverage and sampling bias.

2.9.1 Seawater carbonate system chemistry

For carbonate chemistry data, a high level of quality control (QC) is required because relatively small errors or biases, e.g. a 1 % error in dissolved inorganic carbon (DIC) or total alkalinity (TA), can have important impacts on the determination of seasonal or climatic signals in seawater carbonate chemistry. We therefore used the Global Ocean Data Analysis Project (GLODAPv2) to provide a basic source dataset that has been subject to rigorous QC and bias correction to ensure internal consistency (Key et al., 2015; Olsen et al., 2016). A primary QC flag of 0 (“approximated”), 2 (“good), or 6 (“replicated”) was required for our analyses, and missing time series depth data were calculated from pressure and latitude.

For some carbonate chemistry variables, a significant portion of the available data are “calculated” from measured values of two variables (usually DIC and TA) using a set of equilibrium constants that involves various empirical parameterizations. To test these calculations, we compared calculated vs. measured values of in situ total scale pH by different methods defined by different sets of equilibrium constants (Fig. 20). Calculations were performed using CO2SYS.m (van Heuven et al., 2011) with measured values of DIC, TA, in situ pressure, in situ temperature, salinity, silicate, and phosphate. For all calculation methods, there appears to be significant bias (>0.05 pH units) between measured and calculated values for water samples with salinity (S) lower than around 25 psu. This may be due to bias in both the calculation methods and in the measured values, in part due to pH scale conversions (see Olsen et al., 2016). Until this bias is understood and/or corrected we recommend caution in the use of these calculation methods for Arctic seawater samples with S<25 psu. For S>25 psu, the calculation method using Millero 2010 constants shows best overall agreement with measurements (lowest root-mean-square error), although the differences between calculation methods are minor. For S>25 psu and latitudes >40N (as shown in Figure 20) all calculation methods have an accuracy of around 0.02 units (neglecting measurement error).

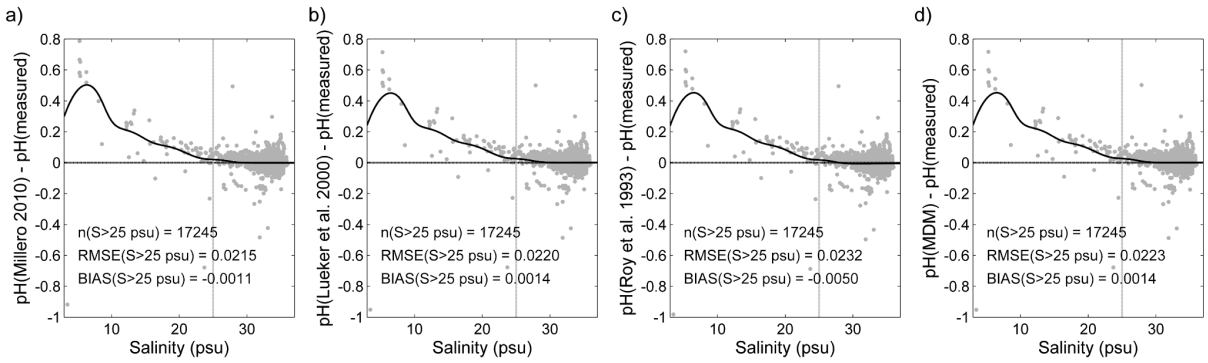

Figure 20. Discrepancies between calculated and measured total scale pH plotted against seawater salinity. Different calculation methods use equilibrium constants from: a) Millero 2010, b) Lueker et al. (2000), c) Roy et al., 1993, d) Mehrbach et al. (1973) refitted by Dickson and Millero (1987). All methods use a sulphate equilibrium constant from Dickson (1990) and total borate from Uppström (1974). Agreement is quantified as root-mean-square error (RMSE) and bias (mean of calculated minus measured) for salinities >25 psu (n = 17245 water samples). Solid lines show kernel smoothings of the discrepancies using a Gaussian kernel with bandwidth 2 psu.

The coverage of the GLODAPv2 data is illustrated for DIC in Fig. 21 and 22 (coverage for other carbonate chemistry variables is broadly similar). Horizontal spatial coverage is relatively patchy with large gaps in parts of the Arctic basins and in the Barents / Kara Seas (Fig. 21 a, the latter can be mitigated by merging in Russian data, but there are QC issues here, see Wallhead et al., 2017). Seasonal coverage favours summer months and especially August/September (Fig. 21 b). Annual coverage favours the late 1990s / early 2000s (Fig. 21c). Vertical coverage, measured as the sampled fraction of water column depth, is generally good in the regions that are sampled (Fig. 22 a). Seasonal coverage, measured as the number of different months of the year sampled, is generally <8 months except at the time series locations in the Icelandic/Norwegian seas and at a hotspot around (75N, 0E) in the Greenland Sea (Fig. 22 b). Annual coverage rarely exceeds 10 unique sampled years except near the Iceland Sea and Irminger Sea time series locations (Fig. 22 c).

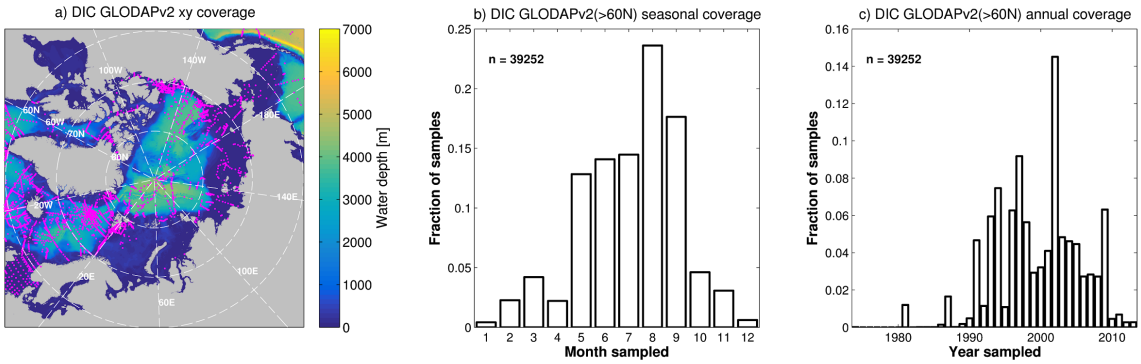

Figure 21. Coverage of in situ dissolved inorganic carbon data from GLODAPv2 data product. a) shows spatial locations of data profiles in the Arctic region (magenta dots, background color shows water depth); b) and c) show the distribution of sampling effort over months and years, for the n = 39252 data at latitudes >60N

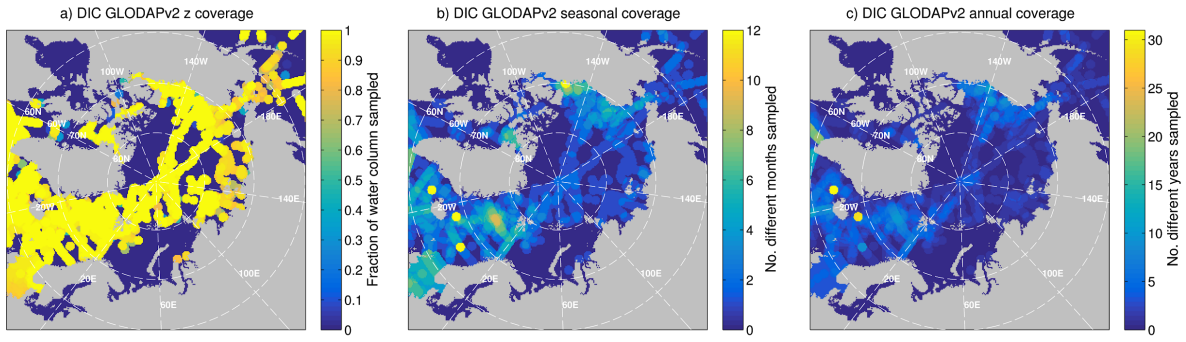

Figure 22. Horizontal variation in dissolved inorganic carbon data coverage from GLODAPv2 data product. a) shows the range of sampled depths relative to the local water depth within a 100 km horizontal radius of each grid point; b) and c) show the number of unique months and years sampled within a 100 km horizontal radius of each grid point.

2.9.2 Seawater nutrients and phytoplankton biomass

The World Ocean Database (WOD, Boyer et al., 2013; Zweng et al., 2018) provides the most comprehensive in situ data compilation for nutrients and phytoplankton biomass as chlorophyll *a*. At the present time (16/04/2018) there are still some data found in ICES and GLODAPv2 compilations that are not yet included in WOD, but these are a minor fraction of the WOD dataset and we understand that they will be soon incorporated in the next WOD release. To our knowledge, the WOD QC procedures are adequate for these variables for most purposes, although for nutrients a higher level of QC (but lower level of coverage) is available from GLODAPv2 (see above).

The WOD Arctic datasets for nutrients (nitrate, phosphate, silicate, oxygen) are roughly an order of magnitude larger than GLODAPv2 carbonate chemistry variables and the spatial coverage is much better, although there are still notable gaps in the Arctic basins (Fig. 23 a shows coverage for nitrate, other nutrients show similar patterns). Sampling effort is again biased towards summer months but the wintertime coverage is better, considering all latitudes >60 N as a whole (Fig. 23b). Annual sampling effort is concentrated around the late 1980s / early 1990s (Fig. 23c).

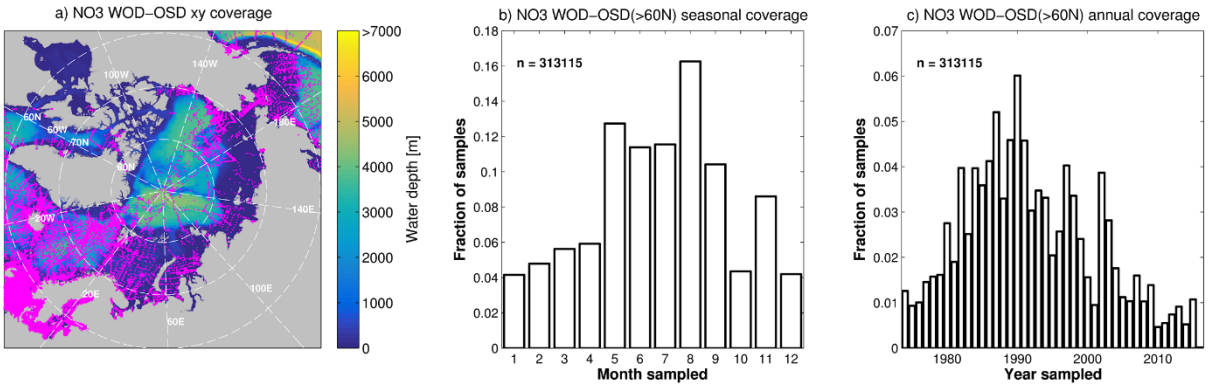

Figure 23. Coverage of in situ nitrate data from WOD-OSD. a) shows spatial locations of data profiles in the Arctic region (magenta dots, background color shows water depth); b) and c) show the distribution of sampling effort over months and years, for the n = 313115 data at latitudes >60N with QC flag = 0 ("accepted value").

Vertical coverage is generally good (Fig. 24a) and seasonal coverage is good (>10 months) for most of the Nordic and Barents Seas, but declines to <6 months on the Russian shelves and in the Canadian Archipelago and Arctic Basin, and rarely exceeds 8 months in the Pacific sector (Fig. 24b). Annual coverage is excellent in the Baltic and North Sea, covering almost all of 43 years within the extraction window (1974-2016), but this declines to <30 years in the Nordic and Barents Seas, and is generally <15 years in other Arctic regions.

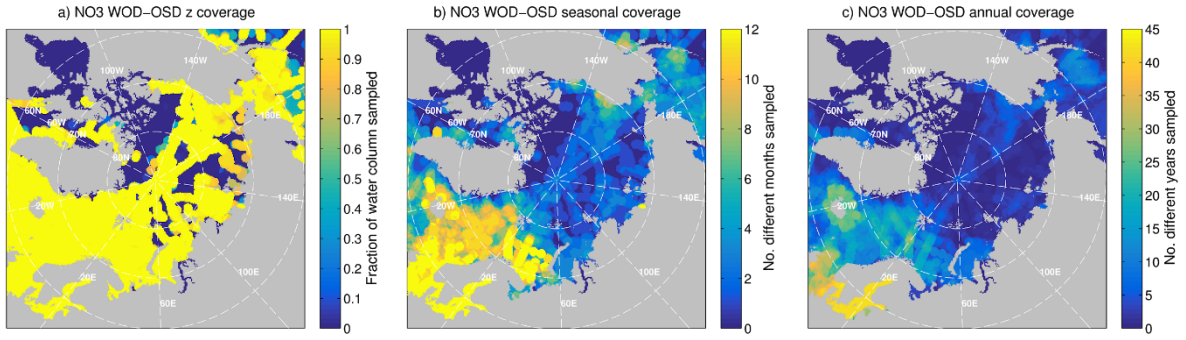

Figure 24. Horizontal variation in nitrate data coverage from the WOD-OSD data collection. a) shows the range of sampled depths relative to the local water depth within a 100 km horizontal radius of each grid point; b) and c) show the number of unique months and years sampled within a 100 km horizontal radius of each grid point.

The WOD Arctic dataset for chlorophyll *a* (Chl) is around a factor of four smaller than for nutrients (Fig. 25) and appears to lack QC-approved data for large stretches of the Arctic basins and Russian shelves (Fig. 25a). The sampling effort is more strongly biased towards summer months (Fig. 25b) and most of the data are from the late 1980s through mid 2000s (Fig. 25c), in particular during 1991 when almost a quarter of the total samples were taken.

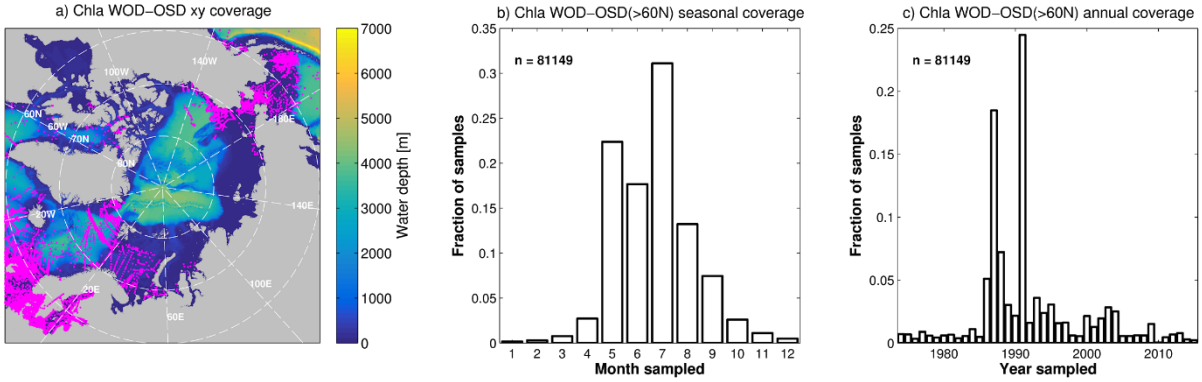

Figure 25. Coverage of in situ chlorophyll data from WOD-OSD. a) shows spatial locations of data profiles in the Arctic region (magenta dots, background color shows water depth); b) and c) show the distribution of sampling effort over months and years, for the n = 81149 data at latitudes >60N with QC flag = 0 ("accepted value").

Vertical coverage is less complete than for nutrients (Fig. 26a), but this is expected since significant chlorophyll concentrations are usually only found in surface (euphotic) waters. Similarly, seasonal coverage is more restricted (Fig. 26b) but may be adequate for the limited growing seasons at high latitudes, except where there are obvious gaps in the spatial coverage (Fig. 25a). Annual coverage is generally <15 years except in parts of the North Sea, Skagerrak, and Baltic (Fig. 26c).

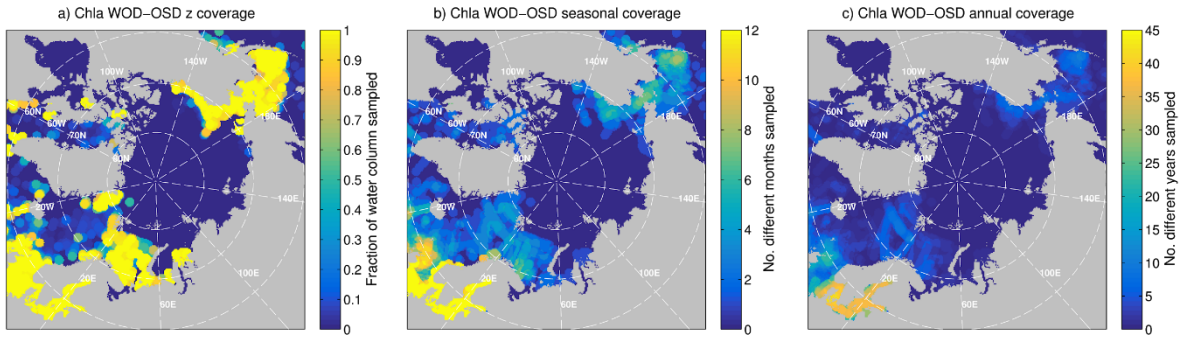

Figure 26. Horizontal variation in chlorophyll data coverage from the WOD-OSD data collection. a) shows the range of sampled depths relative to the local water depth within a 100 km horizontal radius of each grid point; b) and c) show the number of unique months and years sampled within a 100 km horizontal radius of each grid point.

References

Boyer, T. P. et al. (2013), World Ocean Database 2013, Sydney Levitus, Ed.; Alexey Mishonoc, Tech. Ed., NOAA Atlas(72), 209 pp, https://doi.org/10.7289/V5NZ85MT.

Dickson, A. G. (1990), Standard potential of the reaction: AgCl(s) + 12H2(g) = Ag(s) + HCl(aq), and and the standard acidity constant of the ion HSO4– in synthetic sea water from 273.15 to 318.15 K, *J. Chem. Thermodyn.*, *22*(2), 113–127.

Dickson, A. G. and Millero, F. (1987): A comparison of the equilibrium constants for the dissociation of carbonic acid in seawater media, Deep-Sea Res., 34, 1733–1743.

Hastie, T., R. Tibshirani, and J. Friedman (2009), The Elements of Statistical Learning: Data Mining, Inference, and Prediction., 2nd ed., Springer-Verlag, New York.

van Heuven, S., D. Pierrot, J. W. B. Rae, E. Lewis, and D. W. R. Wallace (2011), MATLAB Program Developed for CO2 System Calculations. ORNL/CDIAC-105b. Carbon Dioxide Information Analysis Center, Oak Ridge National Laboratory, U.S. Department of Energy, Oak Ridge, Tennessee., doi:10.3334/CDIAC/otg.CO2SYS_MATLAB_v1.1.

Key, R. M., Olsen, A., van Heuven, S., Lauvset, S. K., Velo, A., Lin, X., . . . Suzuki, T. (2015). Global ocean data analysis project, Version 2 (GLODAPv2) (ORNL/CDIAC-162, ND-P093). Oak Ridge, TN: Carbon Dioxide Information Analysis Center, Oak Ridge National Laboratory, U.S. Department of Energy. https://doi.org/10.3334/CDIAC/OTG.NDP093_GLODAPv2

Lueker, T. J., Dickson, A. G., and Keeling, C. D. (2000): Ocean pCO2 calculated from dissolved inorganic carbon, alkalinity, and equations for K1 and K2: validation based on laboratory measurements of CO2 in gas and seawater at equilibrium, Mar. Chem., 70, 105–119.

Mehrbach, C., Culberson, C. H., Hawley, J. E., and Pytkowicz, R. M. (1973): Measurement of the apparent dissociation constants of carbonic acid in seawater at atmospheric pressure, Limnol. Oceanogr., 18, 897–907.

Millero, F. J. (2010). Carbonate constants for estuarine waters. Marine and Freshwater Research, 61, 139–142.

Olsen, A., Key, R. M., van Heuven, S., Lauvset, S. K., Velo, A., Lin, X., . . . Suzuki, T. (2016). The Global Ocean Data Analysis Project version 2 (GLODAPv2)—An internally consistent data product for the world ocean. Earth System Science Data, 8, 297–323. https://doi.org/10.5194/essd-8-297-2016.

Roy, R. N., Roy, L. N., Vogel, K. M., Porter-Moore, C., Pearson, T., Good, C. E., Millero, F. J., and Campbell, D. M.: The dissociation constants of carbonic acid in seawater at salinities 5 to 45 and temperatures 0 to 45 C, Mar. Chem., 44, 249–267, 1993.

Uppström, L. R. (1974). The boron/chlorinity ratio of deep-sea water from the Pacific Ocean. Deep-Sea Research and Oceanographic Abstracts, 21(2), 161–162.

Wallhead, P.J., Bellerby, R.G.J., Silyakova, A., Slagstad, D., Polukhin, A.A. (2017), Bottom water acidification and warming on the western Eurasian Arctic shelves: Dynamical downscaling projections, Journal of Geophysical Research, Oceans, 122, 8126–8144. doi:10.1002/2017JC013231.

Zweng, M. M., Boyer, T. P., Baranova, O. K., Reagan, J. R., Seidov, D., and Smolyar, I. V.: An inventory of Arctic Ocean data in the World Ocean Database, Earth Syst. Sci. Data, 10, 677-687, https://doi.org/10.5194/essd-10-677-2018, 2018.

3. Recommendations and further work

The data sets described in this report are all characterized as data collection that are built up over many years and are therefore important for studies of changes in ocean and sea ice over decades. As part of INTAROS the processing and management of these data sets are improved, enabling them be become part of an interoperable Arctic observing system, which will be developed under INTAROS. The data sets will continue to be improved and updated with new observations as they become available in the coming years. This includes new data that will be collected as part of WP3 as well as data from other repositories that have not been included in D2.1 and D2.2.

In order to build up sustainable Arctic observing systems, it is necessary to have reliable platforms and instrument for data collection as well as robust processing chains to produce the ocean and sea ice data products. This includes efforts to increase the maturity of all the components of the observing systems, which was assessed in D2.1. Best practices need to be established for the ocean observing systems, and initiatives have started through establishment of a Best practice working group for the ocean. This group includes members from the AtlantOS and the INTAROS projects.

A key challenge in INTAROS is to advance the interoperability between the distributed observing systems. This requires that the data repositories to be used in WP5 must facilitate machine-to-machine communication allow search and downloading of data to be used in the application studies (WP6). The work described in D2.1 and this report will be background for Task 2.3 where selected data sets will be accessed from distributed repositories for interaction in WP5. The work will include harmonization of protocols of the repositories. This includes standardized metadata, identification of existing processing chains and tools, and provision of comprehensive data management routines.

Recommendation for work to follow up the results in D2.1 and D2.2 include:

1) The data sets presented in this report (and other existing data sets that will be needed for the work in WP5 and WP6) must be made available in data repositories that can be accessed from the integrated Arctic observing system in WP5. The data providers must decide which data repositories they will use, preferable existing and well-functioning ones.

2) New data sets, in particular the data coming from new field work in WP3, must be deposited in the same repositories as in 1)

3) Establish dialogue with stakeholder representatives in WP6 to decide which data are most important and most easily accessible form the repositories

4) Collaborate with other projects and other data repositories to ensure that INTAROS follows best practice in developing integrated Arctic observing systems.

4. References

AON Design and Implementation Task Force, 2012, Designing, Optimizing, and Implementing an Arctic

Observing Network (AON): A Report by the AON Design and Implementation (ADI) Task Force.

Study of Environmental Arctic Change (SEARCH), Fairbanks, Alaska. 64 pp.

Atkinson, C., 2015: Ice Thickness Data, ERA-CLIM2 Deliverable D3.16, Report. http://www.era-clim.eu/ERA-CLIM2/Products/

Eicken, H. et al., 2013: Dual-purpose Arctic observing networks: Lessons from SEARCH on frameworks for prioritization and coordination, White paper for Arctic Observing Summit, Vancouver, BC, Canada.

GAIA-CLIM measurement maturity Matrix Guidance, 2015: Task 1.1: Report on system of systems approach adopted and rationale.

Haimberger et al., 2015: Bias adjustments for radiosonde temperature, wind and humidity from existing reanalysis feedback, ERA-CLIM2 Deliverable 4.1, Report. http://www.era-clim.eu/ERA-CLIM2/Products/

Lee, O., H. Eicken, G. Kling, C. Lee, 2015. A Framework for Prioritization, Design and Coordination of Arctic Long-term Observing Networks: A Perspective from the U.S. SEARCH Program. ARCTIC VOL. 68, SUPPL. 1 (2015) http://dx.doi.org/10.14430/arctic4450.

Polar View, 2016. Polaris: Next Generation Observing Systems for the Polar Regions. D2.1 Gaps and Impact Analysis Report, ESA, pp 180.

WMO, 2015: List of all requirements. From OSCAR Observing systems Capability Analysis and Review Tool: https://www.wmo-sat.info/oscar/requirements

http://vocab.ndg.nerc.ac.uk/list/L201/current

https://science.nasa.gov/earth-science/earth-science-data/data-processing-levels-for-eosdis-data-products

---------- END of DOCUMENT----------

INTAROS

This report is made under the project
Integrated Arctic Observation System (INTAROS)
funded by the European Commission Horizon 2020 program
Grant Agreement no. 727890.

Project partners: